AMERICAN SOCIETY FOR MICROBIOLOGY | Molecular and Cellular Biology®

RESEARCH ARTICLE

Eya2, a Target Activated by Plzf, Is Critical for *PLZF-RARA*-Induced Leukemogenesis

Ryoichi Ono,[a] Masahiro Masuya,[b] Satomi Ishii,[a] Naoyuki Katayama,[b] Tetsuya Nosaka[a]

Department of Microbiology and Molecular Genetics[a] and Department of Hematology and Oncology,[b] Mie University Graduate School of Medicine, Tsu, Mie, Japan

ABSTRACT PLZF is a transcription factor that confers aberrant self-renewal in leukemogenesis, and the *PLZF-RARA* fusion gene causes acute promyelocytic leukemia (APL) through differentiation block. However, the molecular mechanisms of aberrant self-renewal underlying *PLZF*-mediated leukemogenesis are poorly understood. To investigate these mechanisms, comprehensive expression profiling of mouse hematopoietic stem/progenitor cells transduced with *Plzf* was performed, which revealed the involvement of a key transcriptional coactivator, Eya2, a target molecule shared by *Plzf* and *PLZF-RARA*, in the aberrant self-renewal. Indeed, *PLZF-RARA* as well as *Plzf* rendered those cells immortalized through upregulation of *Eya2*. *Eya2* also led to immortalization without differentiation block, while depletion of *Eya2* suppressed clonogenicity in cells immortalized by *PLZF-RARA* without influence on differentiation and apoptosis. Interestingly, cancer outlier profile analysis of human samples of acute myeloid leukemia (AML) in The Cancer Genome Atlas (TCGA) revealed a subtype of AML that strongly expressed *EYA2*. In addition, gene set enrichment analysis of human AML samples, including TCGA data, showed that this subtype of AML was more closely associated with the properties of leukemic stem cells in its gene expression signature than other AMLs. Therefore, EYA2 may be a target for molecular therapy in this subtype of AML, including *PLZF-RARA* APL.

KEYWORD leukemia

Received 28 October 2016 **Returned for modification** 15 November 2016 **Accepted** 11 April 2017

Accepted manuscript posted online 17 April 2017

Citation Ono R, Masuya M, Ishii S, Katayama N, Nosaka T. 2017. Eya2, a target activated by Plzf, is critical for *PLZF-RARA*-induced leukemogenesis. Mol Cell Biol 37:e00585-16. https://doi.org/10.1128/MCB.00585-16.

Address correspondence to Ryoichi Ono, onor-tky@umin.net, or Tetsuya Nosaka, nosaka@doc.medic.mie-u.ac.jp.

Oncogenic transformation in malignancy is a multistep process that generates cancer-initiating/stem cells through accumulation of genetic mutations (1). One of the essential steps is aberrant acquisition of self-renewal capacity, which is intrinsically orchestrated by several transcription factors in a context-dependent manner (2). Deregulation of this class of transcription factors is closely associated with various cancers, including hematological malignancies (3, 4).

The *promyelocytic leukemia zinc finger* gene (*PLZF* [also called *ZBTB16*]) encodes a multifunctional transcription factor that regulates gene expression positively through promoter binding (5), as well as negatively through recruitment of polycomb group proteins and histone deacetylases to target promoter regions (6). Previous studies (5, 7) showed that *PLZF* is strongly expressed in hematopoietic stem cells (HSCs) and immature progenitors. While *Plzf* is essential for self-renewal in spermatogenesis, it is not indispensable for normal hematopoiesis (8), but is involved in control of HSC homeostasis (9). In malignant hematopoiesis, we found that Plzf is critically involved in the aberrant self-renewal program induced by *mixed lineage leukemia* (*MLL*) fusion oncogenes (10).

PLZF is also one of the partner genes (*X* genes) that fuse with the retinoic acid (RA) receptor α gene (*RARA*) in chromosomal translocations involving *RARA*, which are characteristic of acute promyelocytic leukemia (APL) (11, 12). Previous studies (13–15)

suggested a model in which an X-RARA fusion oncoprotein dimerizes/oligomerizes via the dimerization domain of X, associates with retinoid X receptor (RXR), and assembles into transcriptional repressor complexes, including transcriptional corepressors and histone deacetylases. In this model, X-RARA complexes repress RA-induced activation of RARA target genes by binding to DNA via the RARA moiety in a dominant-negative manner. In APL, since RARA signaling is critically involved in myeloid differentiation, X-RARA is likely to induce a differentiation block at the promyelocytic stage during myelopoiesis, and supraphysiological doses of all-*trans* RA (ATRA) have efficacy against the most typical subtype of APL with promyelocytic leukemia protein gene (*PML*)-*RARA* gene fusion (16, 17). Interestingly, higher doses of ATRA are usually required for cure of patients with *PML-RARA* APL than for induction of differentiation of APL cells (15). Thus, X-RARA may confer other oncogenic properties on APL cells, including aberrant self-renewal and antiapoptotic capacity. In contrast, high doses of ATRA, at which *PLZF-RARA* APL cells can differentiate, do not cure *PLZF-RARA* APL, which has a worse prognosis than *PML-RARA* APL (15). Consistent with this, all transgenic mice harboring *PLZF-RARA* die of leukemia, while only a few of those harboring *PML-RARA* develop lethal leukemia (18). Several studies (19, 20) on PLZF-RARA revealed that the PLZF moiety recruits corepressors and polycomb group proteins in an ATRA-insensitive manner and directly deregulates PLZF target genes to induce leukemia. In addition, reciprocal RARA-PLZF fusion protein also contributes to leukemogenesis (21, 22). However, the molecular basis for induction of aberrant self-renewal capacity by *PLZF-RARA* is unclear.

The *eyes absent homolog 2* (*EYA2*) gene is one of four *EYA* family genes that encode vertebrate homolog proteins of the *Drosophila melanogaster* protein eyes absent (ea) involved in fly eye development (23, 24). EYA has independent tyrosine and threonine phosphatase activities and transactivation potential and is involved in diverse biological functions such as innate immunity, DNA damage repair, and cellular proliferation (24–29). When EYA, which is intrinsically localized in the cytoplasm, interacts with its DNA-binding partner Six via its well-conserved C-terminal domain, the EYA complex is translocated into the nucleus to bind DNA through the Six homeodomain (28, 29). Among mammalian *Eya* genes, only *Eya2* is differentially expressed in mouse long-term HSCs (LT-HSCs), implying an important function associated with HSCs (30). Furthermore, there is accumulating evidence for involvement of EYA2 in tumorigenesis, including clinical findings that *EYA2* is overexpressed in breast and ovarian cancers with a poor prognosis and is required for epithelial-mesenchymal transition (EMT) (31, 32). However, nothing is known about the role of *EYA2* in leukemogenesis.

To unveil the molecular mechanism of *Plzf*-mediated leukemogenesis, we demonstrate upregulation of *Eya2* by Plzf through promoter binding, which was found to be critical for immortalization of hematopoietic stem and/or progenitor cells. Interestingly, *Eya2* was capable of conferring aberrant self-renewal capacity on hematopoietic stem and/or progenitor cells, leading to leukemic immortalization, and human *EYA2* was found to be highly expressed in a subtype of acute myeloid leukemia (AML) by analysis of a public database. We also show that Eya2 is critically involved in the aberrant self-renewal program in *PLZF-RARA*-mediated leukemogenesis, which suggests Eya2 as a novel therapeutic target in *PLZF-RARA* APL.

RESULTS

***Plzf* upregulates *Eya2* expression in the aberrant self-renewal program.** To investigate the molecular basis of *Plzf*-driven aberrant self-renewal, we performed comprehensive gene expression profiling of *Plzf*-transduced c-Kit$^+$ Sca-1$^+$ lineage$^-$ (Lin$^-$) (KSL) and myeloid progenitor (MP) cells using cDNA microarray analysis (GEO accession no. GSE84771) (Fig. 1A). Since *Plzf* is capable of immortalizing both KSL and MP cells (10), we chose genes differentially expressed in the same direction in both cell types, some of which overlapped the genes in the previous report (5) using human cord blood cells transduced with *PLZF*. Among the genes chosen, we focused on *Eya2*, which is known to be associated with HSCs and several malignant tumors, but has not

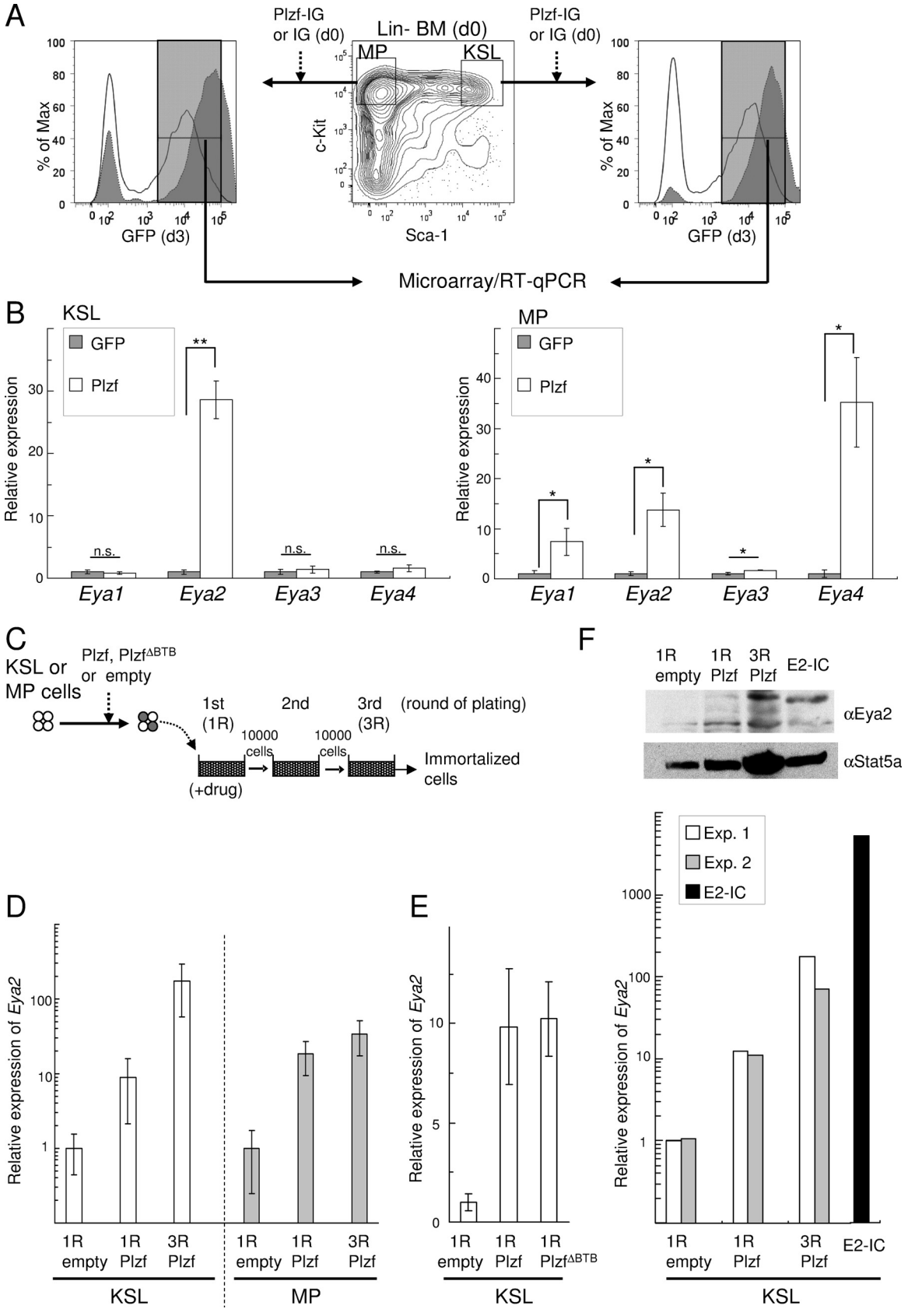

FIG 1 Myeloid immortalization of KSL and MP cells by *Plzf* in association with high *Eya2* expression. (A) Experimental strategy for gene expression profiling of *Plzf*-transduced cells. (Middle panel) Lin-depleted (Lin$^-$) BM cells displayed with the sorting gate for KSL and MP cells. Both subpopulations were retrovirally transduced with *Plzf*-IRES-*EGFP* (Plzf-IG) or *EGFP* (empty [IG]), in pMYs-IG on day 0 (d0). (Left

(Continued on next page)

been investigated in leukemogenesis. Reverse transcription-quantitative PCR (RT-qPCR) analyses showed that *Eya2* expression was significantly higher in *Plzf*-transduced KSL and MP cells, while expression of the family genes *Eya1*, *Eya3*, and *Eya4* was higher only in transduced MP cells (Fig. 1B). In myeloid immortalization assays using *Plzf*-transduced cells (Fig. 1C), *Eya2* expression was higher in transduced colony-forming cells and was enhanced with serial replating in KSL-derived cells (Fig. 1D). Interestingly, *Eya2* expression was also increased in the KSL cells transduced with a *Plzf* mutant lacking the BTB/POZ domain (Plzf$^{\Delta BTB}$) (Fig. 1E), which failed to immortalize KSL and MP cells as previously reported (10). An increase in Eya2 protein expression was confirmed (Fig. 1F). The Eya2 protein level was higher in *Eya2*-immortalized KSL cells (described in detail later) than that in *Plzf*-transduced KSL cells (Fig. 1F). These results suggested that induction of *Eya2* expression seemed to correlate with, but was not sufficient for, the *Plzf*-driven immortalization.

Next to examine whether Plzf directly upregulates *Eya2* expression, the three distinct putative transcription start sites (TSSs [in exons 1a, 1b, and 1c, respectively]) of *Eya2* were characterized in the mouse genomic database. Interestingly, chromatin immunoprecipitation sequencing (ChIP-seq) data from the thymus, where expression of *Eya2* as well as *Plzf* is detected (7, 31), revealed that trimethylated histone H3 lysine 4 (H3K4me3) was concentrated in a sharp peak around exon 1c of *Eya2*, accompanied by relatively weak signals of acetylated H3K27 (H3K27ac) and monomethylated H3K4 (H3K4me1), across the genomic region covering the *Eya2* gene and its approximately 74-kb upstream sequence (Fig. 2A). In bone marrow (BM), relatively weak but similar enrichment of the active histone modifications was also found around exon 1c. However, since an enrichment of RNA polymerase II (Pol II) binding was ambiguous around exon 1c, presumably in association with low *Eya2* expression in these normal tissues, RT-PCR analyses of *Plzf*-immortalized KSL cells with primers spanning exons 1a, 1b, or 1c to 4 were performed (Fig. 2A and B). Consistent with the findings on the histone modifications, only a transcript including exons 1c to 4 of *Eya2* was detected (Fig. 2C). These results suggested that transcription of *Eya2* in the *Plzf*-immortalized cells was possibly initiated from the promoter around exon 1c.

Furthermore, ChIP-qPCR assays using KSL and MP cells immortalized by FLAG-tagged-*Plzf* were performed around these three first exons of *Eya2* (Fig. 2B). These analyses showed a significant increase of Plzf binding to the regions upstream of exon 1c in the immortalized cells, accompanied by RNA Pol II binding signals (Fig. 2D). Therefore, these results suggested that Plzf induced *Eya2* expression via promoter binding in immortalization of hematopoietic stem and/or progenitor cells.

***Eya2* can lead to aberrant self-renewal in hematopoietic stem and/or progenitor cells.** To examine whether highly expressed *Eya2* itself may confer an aberrant self-renewing property on hematopoietic stem and/or progenitor cells, KSL and MP cells were retrovirally transduced with *Eya2* and subjected to myeloid immortalization assays (Fig. 3A). Both KSL and MP cells transduced with *Eya2* were immortalized after serial replating (Fig. 3B to E) and generated similar compact colonies (Fig. 3F; data not shown). Morphological and immunophenotypical analyses revealed that most of the cells constituting these KSL (Fig. 3G and H)- and MP (data not shown)-derived immortalized colonies had similar myelomonocytic features without expression of the imma-

FIG 1 Legend (Continued)
[MP] and right [KSL] panels) Green fluorescent protein (GFP)-positive cells (blank area for Plzf-IG, gray shading for IG) were sorted on day 3 (d3). (B) Expression levels of *Eya* family genes in *Plzf*-transduced cells by RT-qPCR normalized to *Actb*. *, $P < 0.05$; **, $P < 0.005$; n.s., not significant. (C) Experimental strategy for myeloid immortalization assays of KSL and MP cells with retroviral transduction of *Plzf* or a *Plzf* mutant lacking its BTB/POZ domain (*Plzf*$^{\Delta BTB}$). pMYs-IRES-*Neomycin*^{r} (pMYs-IN) and pMYs-IRES-*puromycin*^{r} (pMYs-IP) were used as backbone vectors (empty) in panels D and F and panel E, respectively. (D and E) Expression levels of *Eya2* by RT-qPCR normalized to *Actb* in the myeloid immortalization assays of *Plzf*-transduced cells (D) and *Plzf*- or *Plzf*$^{\Delta BTB}$-transduced KSL cells (E), respectively. (F) Expression levels of Eya2 protein (upper) in comparison with those of *Eya2* transcripts (lower). In two independent experiments (Exp. 1 and 2) with the immortalization assays, cell lysates and RNA prepared from colony-forming cells were subjected to Western blotting using anti-Eya2 and anti-Stat5a (an internal control) antibodies (αEya2 and αStat5a) and RT-qPCR analyses, respectively. *Eya2*-immortalized KSL cells (E2-IC [described in detail later]) were used as a positive control. Representative blots (Exp. 1) are shown in the upper panels. Bar graphs show means ± standard deviations (SD) from three independent experiments in panels B, D, and E.

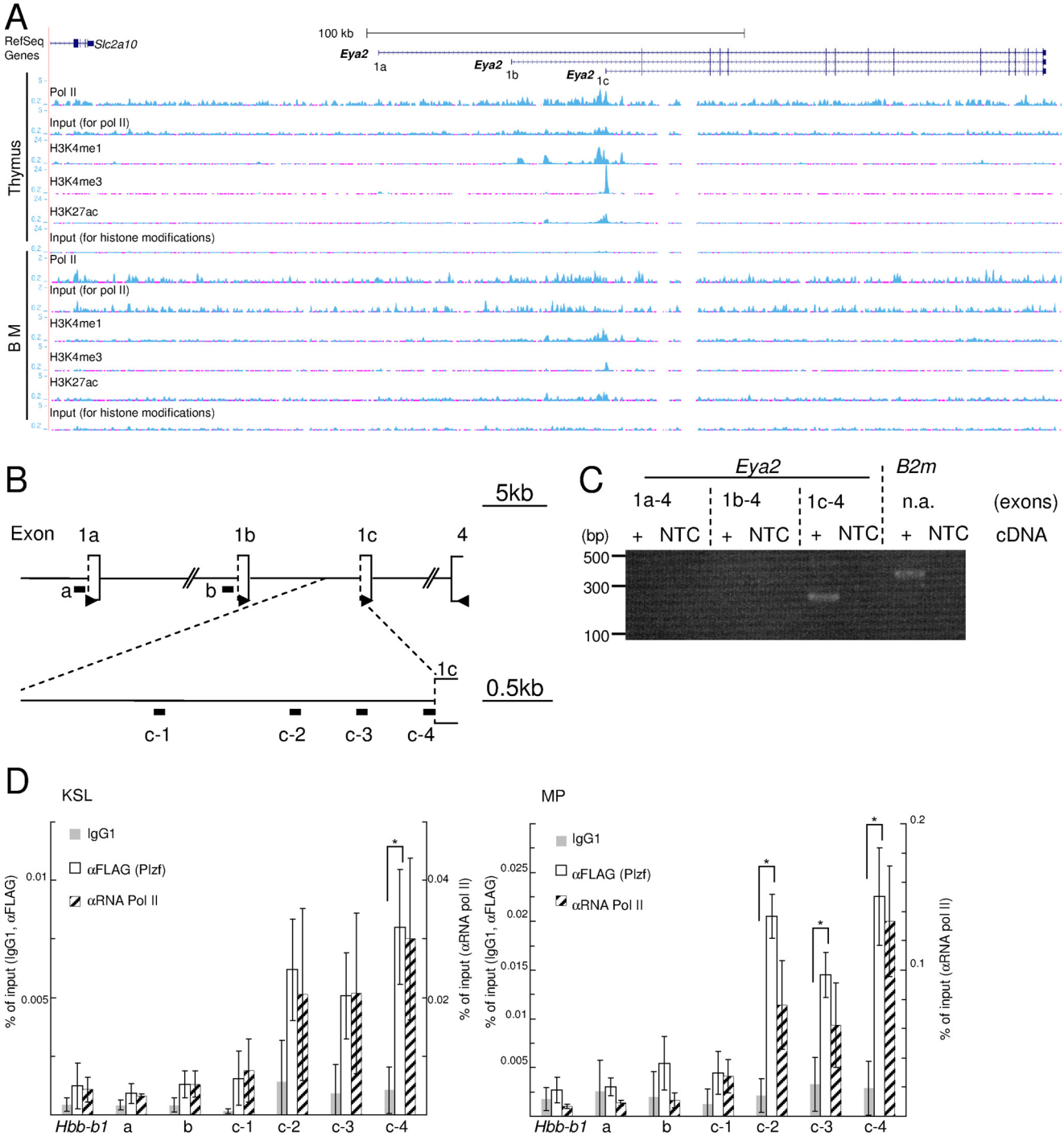

FIG 2 Localization of Plzf in the putative promoter region of *Eya2*. (A) Overview of the genomic region covering *Eya2* and its upstream sequence. In an adapted UCSC Genome Browser view (chromosome 2: 165,333,718 to 165,601,417 [on mm9]), three kinds of *Eya2* transcripts are shown in the RefSeq gene track (top). ChIP-seq data from mouse thymus (middle) and bone marrow (BM) (bottom) are shown in the corresponding LICR TFBS (Pol II and input control) and histone (H3K4me3, H3K4me1, H3K27ac, and input control) tracks. (B) Genomic structure of alternative first exons of *Eya2*. Primer sets (for the regions of a, b, c-1, c-2, c-3, and c-4 in ChIP-qPCR shown in panel D) were designed around these exons. Arrowheads indicate primers detecting alternative transcripts of *Eya2* in panel C. (C) Detection of alternative transcripts of *Eya2* by RT-PCR in *Plzf*-immortalized KSL cells. NTC, negative control. (D) Relative binding of Plzf (detected by anti-FLAG antibody) and RNA polymerase II around exon 1c of *Eya2* in KSL (left) and MP (right) cells immortalized by FLAG-tagged *Plzf*. The promoter region of *Hbb-b1* was examined as a negative control. *, $P < 0.05$. Bar graphs show means ± SD from three independent experiments.

ture surface markers c-Kit and Sca-1, even in KSL-derived colonies. In KSL cells immortalized by FLAG-tagged *Eya2*, the transduced Eya2 was localized in the nucleus and cytoplasm, as previously reported (28, 29) (Fig. 3I). These results suggested that *Eya2* was capable of conferring an aberrant self-renewal capacity on hematopoietic stem and/or progenitor cells without differentiation block in the myeloid lineage.

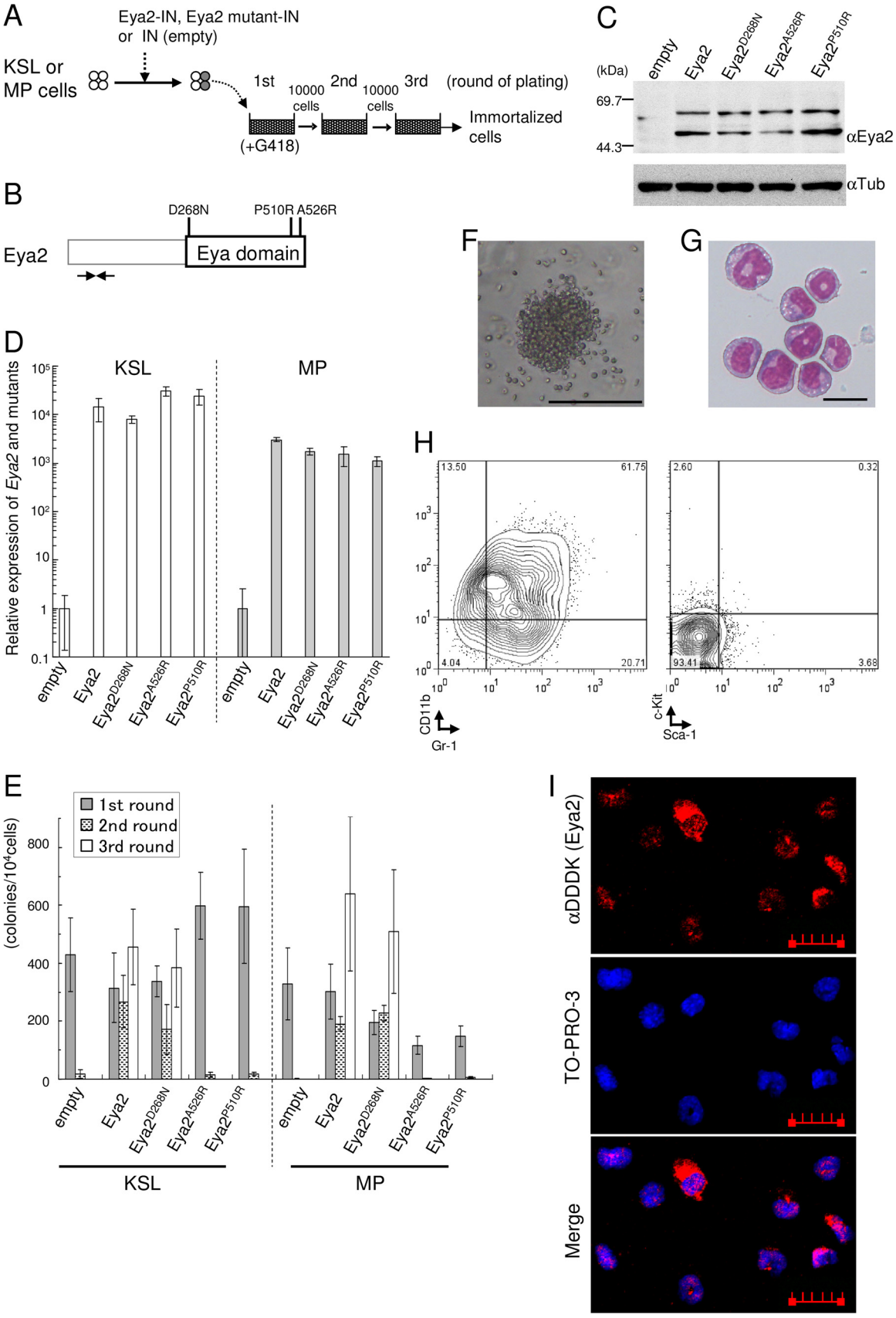

FIG 3 Myeloid immortalization of KSL and MP cells by *Eya2*. (A) Experimental strategy for myeloid immortalization assays with retroviral transduction using pMYs-IN. (B) Structure of Eya2 and missense mutants. Arrows show primers used in RT-qPCR. (C) Expression of Eya2

(Continued on next page)

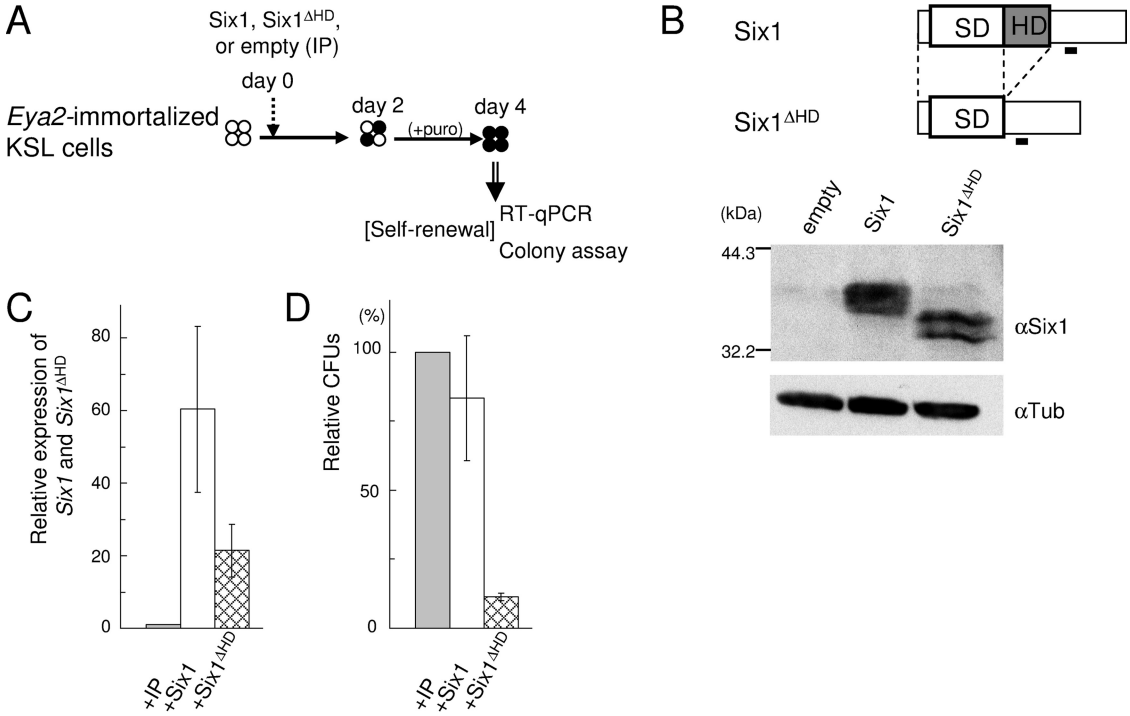

FIG 4 Involvement of *Six1* in myeloid immortalization by *Eya2*. (A) Experimental strategy for analysis of *Eya2*-immortalized KSL cells with retroviral transduction of Six1 or the Six1 mutant lacking its homeodomain (Six1$^{\Delta HD}$) using pMYs-IP. puro, puromycin. (B) Structure of Six1 and Six1$^{\Delta HD}$ and their expression by Western blotting analyses using anti-Six1 antibody (αSix1) and anti-α-tubulin (αTub [an internal control]). Horizontal lines indicate the regions amplified by RT-qPCR. SD, Six domain; HD, homeodomain. (C and D) Expression levels of *Six1* and *Six1*$^{\Delta HD}$ by RT-qPCR (C) and relative CFU (D [3,000 cells/dish]) of the *Eya2*-immortalized cells forced to express Six1 or Six1$^{\Delta HD}$.

To investigate the molecular mechanism of immortalization by *Eya2*, several *Eya2* mutants were generated on the basis of previous findings (24, 33) and subjected to myeloid immortalization assays (Fig. 3A to C). Two mutants (Eya2^{P510R} and Eya2^{A526R}) lacking interaction with a critical homedomain-containing partner, Six1, failed to immortalize KSL and MP cells. Meanwhile, another mutant (Eya2^{D268N}), in which the substitution for an aspartic acid (D268) critical for the tyrosine phosphatase activity was expected to reduce the enzymatic activity, still immortalized (Fig. 3D and E). In addition, retroviral transduction of a Six1 mutant lacking homeodomain (Six1$^{\Delta HD}$) suppressed clonogenicity of *Eya2*-immortalized KSL cells more strongly than that of wild-type Six1 did (Fig. 4).

Furthermore, since Eya resides in the nucleus and cytoplasm and has various functions in association with its localization, a retroviral construct expressing *ER-Eya2* where *Eya2* was fused to the ligand binding domain of the mouse estrogen receptor gene (*ER*) was generated to control the localization and subjected to the myeloid immortalization assays (Fig. 5A to C). Myeloid immortalization of KSL and MP cells was found only in the presence of 4-hydroxytamoxifen (4OHT) (Fig. 5D), and the immortalized cells formed colonies in a 4OHT-dependent manner (Fig. 5E). Immunostaining of

FIG 3 Legend (Continued)
and its mutants by Western blotting analyses using anti-Eya2 and anti-α-tubulin (αTub [an internal control]) antibodies (αEya2 and αTub). (D) Expression levels of *Eya2* and its mutants by RT-qPCR of colony-forming cells at the end of the first plating in panel A. (E) Myeloid immortalization assays of KSL and MP cells after retroviral transduction. (F to H) Typical morphology of colonies of *Eya2*-transduced KSL cells at the third round of plating (F) and typical morphology (G) and immunophenotype (H) of the cells constituting the colonies. Cells were stained with Wright-Giemsa stain. (I) Localization of Eya2 in the FLAG-tagged *Eya2*-immortalized KSL cells analyzed by immunofluorescent confocal microscopy. Alexa Fluor 568-conjugated secondary antibody reacting with anti-DDDDK-tag antibody (αDDDDK) in the immortalized cells visualized their cellular localization (top). Nuclei were visualized with TO-PRO-3 iodide (middle), and a merged image is displayed (bottom). Magnifications (bar lengths): F, $\times$40 (200 μm); G, $\times$400 (20 μm); I, $\times$400 (30 μm). Bar graphs show means $\pm$ SD from three independent experiments.

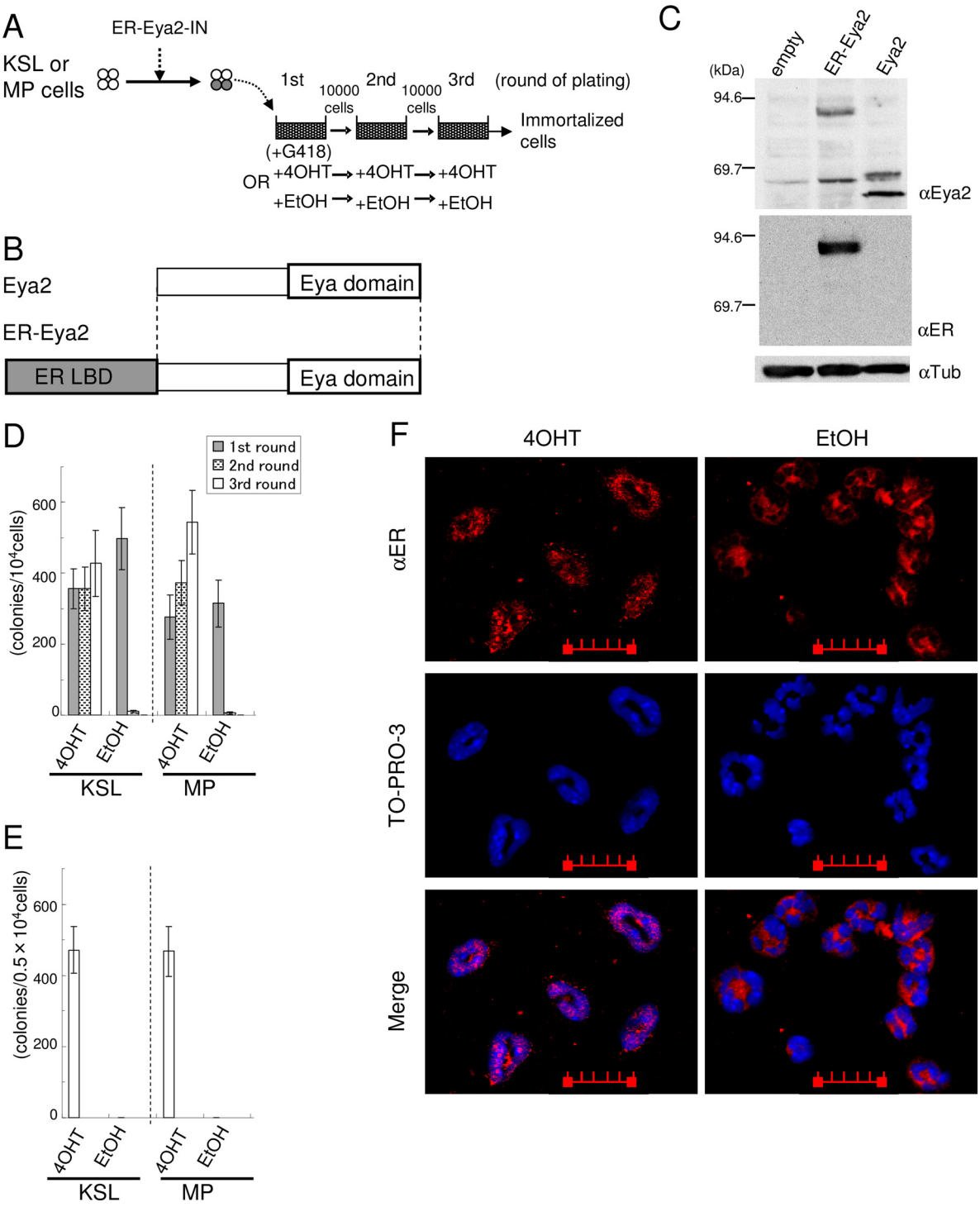

FIG 5 Inducible immortalization of KSL and MP cells by *ER-Eya2*. (A) Experimental strategy for myeloid immortalization assays of KSL and MP cells with retroviral transduction of the *ER-Eya2* fusion gene using pMYs-IN. *ER*, estrogen receptor gene; 4OHT, 4-hydroxytamoxifen. (B) Structure of Eya2 and ER-Eya2. LBD, mutant ligand-binding domain of the mouse ER. (C) Expression of ER-Eya2 by Western blotting using anti-Eya2 (αEya2 [top]), anti-ER antibody (αER [middle]), and anti-α-tubulin (αTub [an internal control; bottom]). (D) Myeloid immortalization assays of *ER-Eya2*-transduced cells in the presence or absence of 4OHT. (E) 4OHT-dependent clonogenicity of cells inducibly immortalized by *ER-Eya2*. (F) Localization of ER-Eya2 in the inducibly immortalized KSL cells analyzed by immunofluorescent confocal microscopy, following a 3-day culture in the presence (left panels) and absence (right panels) of 4OHT. Alexa Fluor 568-conjugated secondary antibody reacting with anti-ER in the immortalized cells visualized its cellular localization (top). Nuclei were visualized with TO-PRO-3 iodide (middle), and merged images are displayed (bottom). Magnification (bar length), ×400 (30 μm). Bar graphs show the means ± SD from three independent experiments.

the immortalized KSL cells confirmed that most of ER-Eya2 was localized in the nucleus in the presence of 4OHT, whereas the majority of ER-Eya2 was exclusively relocated to the cytoplasm in the absence of 4OHT (Fig. 5F). These results suggested that immortalization of hematopoietic stem and/or progenitor cells by Eya2 required the interaction with Six1 in the nucleus and also implied a possibility that the immortalization does not require the full tyrosine phosphatase activity of Eya2.

***PLZF-RARA* upregulates *Eya2* expression in the aberrant self-renewal program.** *PLZF-RARA* shares some target genes with wild-type *PLZF* in leukemogenesis (5, 20). Therefore, Lin/Sca-1-depleted myeloid progenitor cells were retrovirally transduced with *PLZF-RARA*, *PML-RARA*, or *Hoxa9*/*Meis1a*, which immortalizes the myeloid progenitor cells independently of *Plzf* (10) (Fig. 6A and B). RT-qPCR analyses of the transduced cells showed that *Eya2* was highly expressed in *PLZF-RARA*-transduced cells, as in *PLZF*-transduced cells, but not in *Hoxa9*/*Meis1a*-transduced cells (Fig. 6C). *PLZF-RARA* immortalized the myeloid progenitor cells after serial colony replating (19, 20), with maintenance of the *Eya2* expression level, while *Hoxa9*/*Meis1a* immortalized those cells without maintaining the *Eya2* expression level. *PML-RARA*, which is reported to be capable of immortalizing (19), also induced relatively weak *Eya2* expression, compared with that in *PLZF-RARA*-transduced cells (Fig. 6A to C). In contrast, expression levels of other known target genes of *PLZF-RARA*, such as *Bcl2* and c-*Myc*, were not significantly different between *PLZF-RARA*- and *PML-RARA*-transduced cells, while the *Cebpε* expression level was significantly higher in *PLZF-RARA*-transduced cells after serial replating (Fig. 6D). Importantly, *Eya2* expression relative to transgene expression, calculated using the ratio of the copy numbers of each transcript, was significantly higher in *PLZF-RARA*-transduced cells than in *PLZF*-transduced cells (Fig. 6E). Furthermore, degradation of PLZF-RARA by ATRA treatment in *PLZF-RARA*-immortalized cells (Fig. 6F, 19) led to a decrease in *Eya2* expression prior to growth reduction in liquid culture in a time course-dependent manner (Fig. 6G) and also reduced clonogenicity accompanied by a decrease in *Eya2* expression in a dose-dependent manner (Fig. 6H).

Interestingly, our investigation using a public database of comprehensive expression profiling suggested that *EYA2* expression was significantly higher in *PLZF-RARA* APL (22) than that in *PML-RARA* APL (34), although cancer outlier profile analysis (COPA) transformation of data from another cohort (35) showed a few *PML-RARA* APL cases with relatively high *EYA2* expression (Fig. 7).

Eya2 is critically involved in myeloid immortalization by *PLZF-RARA in vitro*. To corroborate the role of *Eya2* in myeloid immortalization by *PLZF-RARA*, *Eya2* was depleted in *PLZF-RARA*-immortalized cells by short hairpin RNA (shRNA) expression. First, effects of two shRNAs were examined in the cells with forced expression of *Eya2* (Fig. 8). Then, the functional role of Eya2 was analyzed in the *PLZF-RARA*-immortalized cells using these two shRNAs. Both shRNAs effectively depleted endogenous *Eya2* expression, and both reduced clonogenicity to about 60% of that in the control (Fig. 9A to C). To investigate the molecular mechanism, we examined the expression levels of several known target genes of *PLZF-RARA* in the immortalized cells with *Eya2* depletion at the time when the depletion may have caused changes (Fig. 9A). However, expression levels were not significantly affected (Fig. 9D), and fluorescence-activated cell sorter (FACS) analyses showed little effect on differentiation and apoptosis (Fig. 9E). We also confirmed restoration of the reduced clonogenicity with forced expression of shRNA-resistant *Eya2* lacking the shRNA target regions (Fig. 10). These results suggested that *PLZF-RARA* might confer an aberrant self-renewal potential on myeloid progenitor cells, leading to immortalization *in vitro*, at least partly through upregulation of *Eya2*. In addition, we found that *Eya2* depletion by shRNA led to reduction of clonogenicity in the *Plzf*-immortalized (Fig. 11A to C) and *PML-RARA*-immortalized cells (Fig. 11D to F).

To further clarify the role of *Eya2* in immortalization by *PLZF-RARA*, we focused on the dual phosphatase activities of Eya2. Concerning the threonine phosphatase activity of Eya2, a recent study (36) showed that Eya1, which is homologous to Eya2, can stabilize c-Myc through dephosphorylation of phosphothreonine 58 (pT58) during

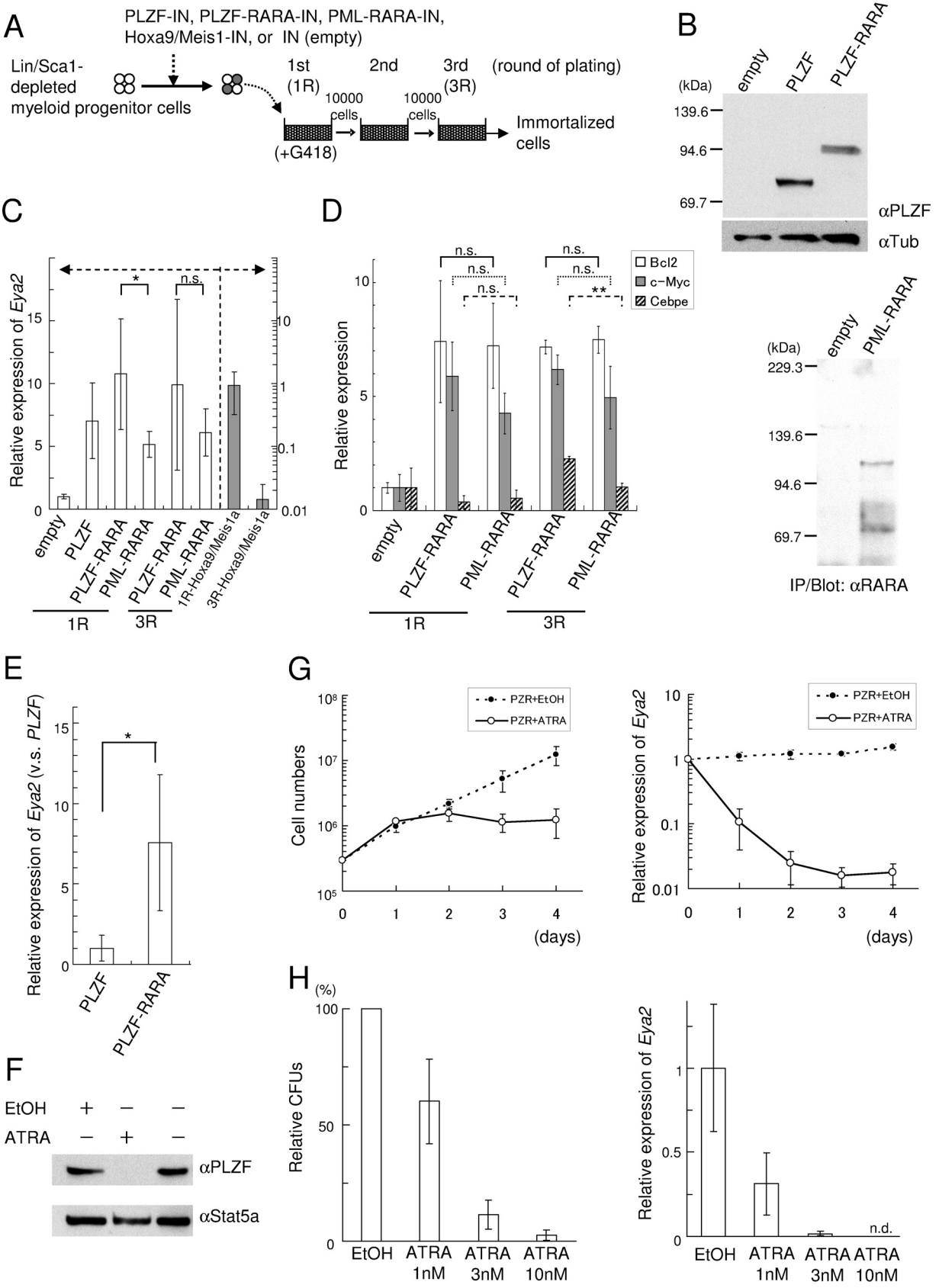

FIG 6 Myeloid immortalization of myeloid progenitor cells by *PLZF-RARA* in association with *Eya2* expression. (A) Experimental strategy for myeloid immortalization assays of Sca-1/Lin-depleted myeloid progenitor cells. The cells were retrovirally transduced with *PLZF*, *PLZF-RARA*, *PML-RARA*, and *Hoxa9*-IRES-*Mesi1* (*Hoxa9*/*Meis1*) in pMYs-IN. (B) Expression of PLZF, PLZF-RARA, and PML-RARA by Western blotting analyses.

(Continued on next page)

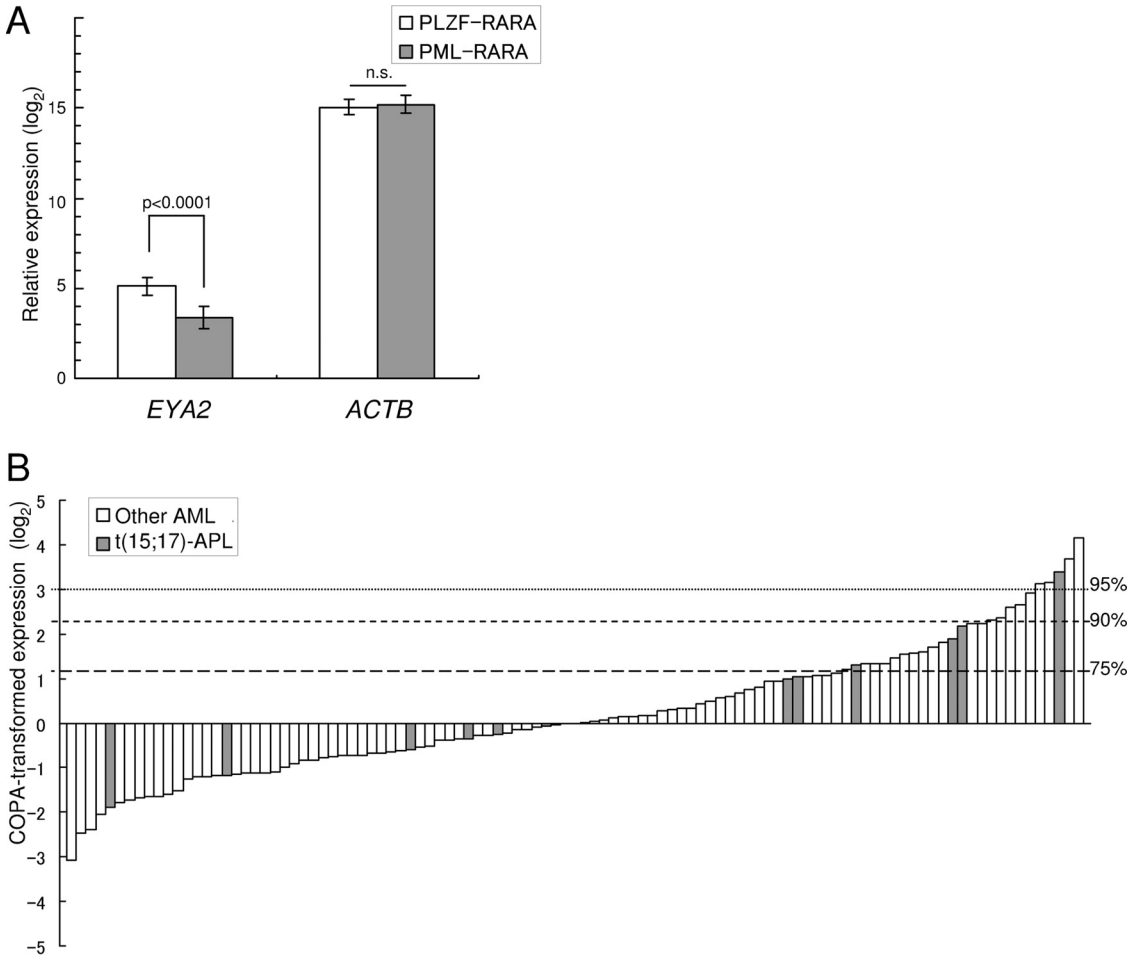

FIG 7 Expression levels of *EYA2* in human leukemia samples. (A) Expression levels of *EYA2* and *ACTB* in normalized *PLZF-RARA* APL (n = 5 [GSE8510]) and *PML-RARA* APL (n = 15 [GSE61804]) samples. (B) Waterfall plot of COPA-transformed expression levels of *EYA2* in AML (n = 105 [GSE12662]) samples, including t(15;17) APL (n = 13) samples.

nephrogenesis. Since Eya2 was preliminarily found to associate with pT58-c-Myc by coimmunoprecipitation analysis in 293T cells (data not shown), we examined expression levels of total c-Myc and pT58-c-Myc in *PLZF-RARA*-immortalized cells with *Eya2* depletion, but found no significant changes (Fig. 12).

Taken together, these results suggested that Eya2 had a crucial role in the aberrant self-renewal activity conferred by *PLZF-RARA in vitro*, independent of posttranslational modification of c-Myc.

A human AML subtype with upregulated *Eya2* has an LSC expression signature. Finally, to examine the involvement of *Eya2* in human AML, we performed COPAs of the Oncomine database. COPAs of AML gene expression data in TCGA revealed that *Eya2* was highly expressed in a subtype of AML (Fig. 13A). Since *Eya2* expression was not

FIG 6 Legend (Continued)

Lysates extracted from Plat E cells transfected with empty vector (pMYs-IN), pMYs-PLZF-IN, or pMYs-PLZF-RARA-IN were blotted with anti-PLZF antibody (αPLZF), followed by being reprobed with anti-α-tubulin antibody (αTub) as an internal control (upper panels). Lysates extracted from Plat E cells transfected with empty (pMYs-IN) or pMYs-PML-RARA-IN were immunoprecipitated with anti-RARA antibody (αRARA), followed by blotting with anti-RARA (lower panel). (C and D) Expression levels of *Eya2* (C) and *Bcl2*, *c-Myc*, and *Cebpε* (D) by RT-qPCR in the myeloid immortalization assays. (E) Relative expression levels of *Eya2* by RT-qPCR in the retrovirally transduced cells at the end of the first plating. Normalization was performed using primers for a part of the *PLZF* portion of *PLZF-RARA*. (F) Degradation of PLZF-RARA by ATRA in *PLZF-RARA*-immortalized cells by Western blotting analyses. Lysates extracted from these cells with 1 μM ATRA or vehicle control (EtOH) for 16 h were blotted with anti-PLZF, followed by being reprobed with anti-Stat5a as an internal control. (G) Time course of cell proliferation (left) and expression levels of *Eya2* by RT-qPCR (right) in *PLZF-RARA*-immortalized cells with 1 μM ATRA or vehicle control (EtOH). (H) Effect of ATRA on clonogenicities (3,000 cells/dish [left]) and expression levels of *Eya2* by RT-qPCR (right) in *PLZF-RARA*-immortalized cells. Bar graphs show means ± SD from three independent experiments. *, $P < 0.05$; **, $P < 0.005$; n.s., not significant.

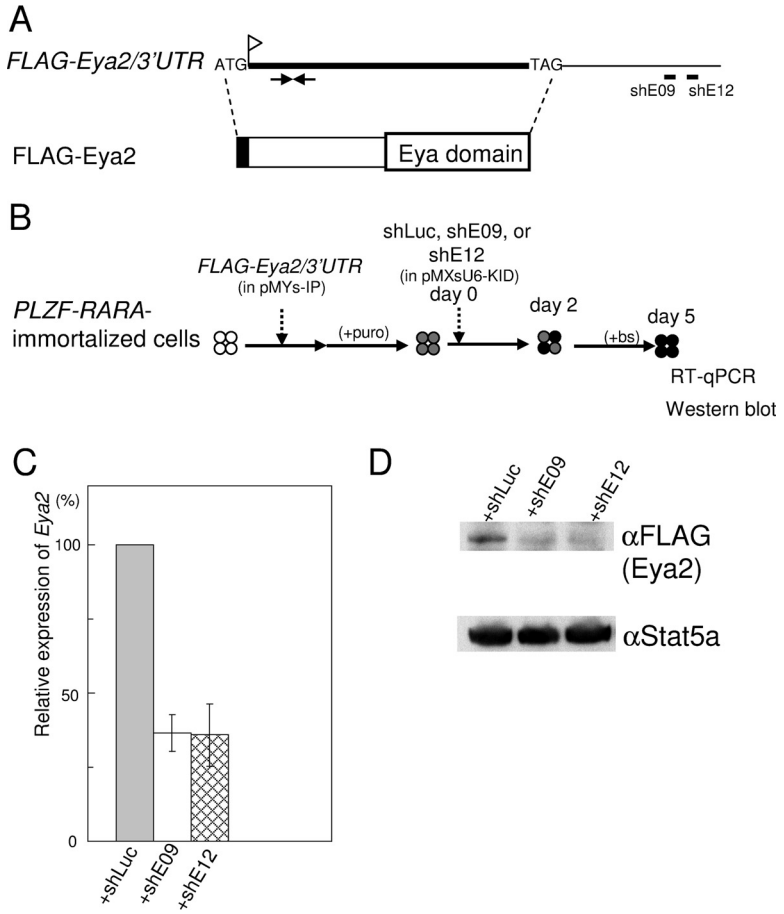

FIG 8 Evaluation of knockdown effects of shRNAs against *Eya2*. (A) Schematic representation of N-terminally FLAG-tagged *Eya2* ligated to a part of the 3′ UTR (*FLAG-Eya2/3′UTR*) containing target sequences for two shRNAs (shE09 and shE12). The coding sequence of *Eya2* except for the first ATG and the partial sequence of the 3′ UTR are shown in thick and thin horizontal lines, respectively. A flag and a black box indicate the FLAG sequence and peptides, respectively. Arrows indicate primers used in RT-qPCR. (B) Experimental strategy for shRNA-mediated *Eya2* depletion in *PLZF-RARA*-immortalized cells forced to express FLAG-Eya2. *PLZF-RARA*-immortalized cells were retrovirally transduced with *FLAG-Eya2/3′* UTR in pMYs-IP. Following puromycin (puro) selection for 3 days, the cells expressing *FLAG-Eya2/3′* UTR were next retrovirally transduced with shRNA expressors in pMXsU6-KID. bs, blasticidin; shLuc, shRNA against the *luciferase* gene. (C and D) Expression levels of *Eya2* transcripts by RT-qPCR (C) in comparison with those of FLAG-Eya2 protein by Western blotting analyses (D) in the *PLZF-RARA*-immortalized cells expressing *FLAG-Eya2/3′* UTR after shRNA transduction. Lysates extracted from the shRNA-transduced cells were blotted with anti-FLAG antibody (αFLAG), followed by reprobe with anti-Stat5a as an internal control. Bar graphs show means ± SD from three independent experiments.

related to clinical features, including the French-American-British (FAB) classification of AML (data not shown), we performed gene set enrichment analyses (GSEAs) of a TCGA AML cohort using the top ($EYA2^{high}$) and bottom ($EYA2^{low}$) 5th percentile samples to characterize the molecular basis of this subtype of AML. The results showed significant enrichment of leukemic stem cell (LSC)-associated downregulated genes (37) in the $EYA2^{low}$ group (Fig. 13B), but LSC-associated upregulated genes were not significantly enriched in the $EYA2^{high}$ group. Meanwhile, significant enrichment of LSC-associated upregulated genes in cases with high *EYA2* expression (38) was found in another AML cohort (accession no. GSE61804) (34) (Fig. 13C). Interestingly, GSEAs of the TCGA and GSE61804 cohorts also showed significant enrichment of mouse LT-HSC-associated genes (39) in the $EYA2^{high}$ group and in cases with high *EYA2* expression, respectively (Fig. 13D; data not shown). These results suggested a possible subtype of human AML with high *EYA2* expression that is associated with an aberrant self-renewal activity in LSCs.

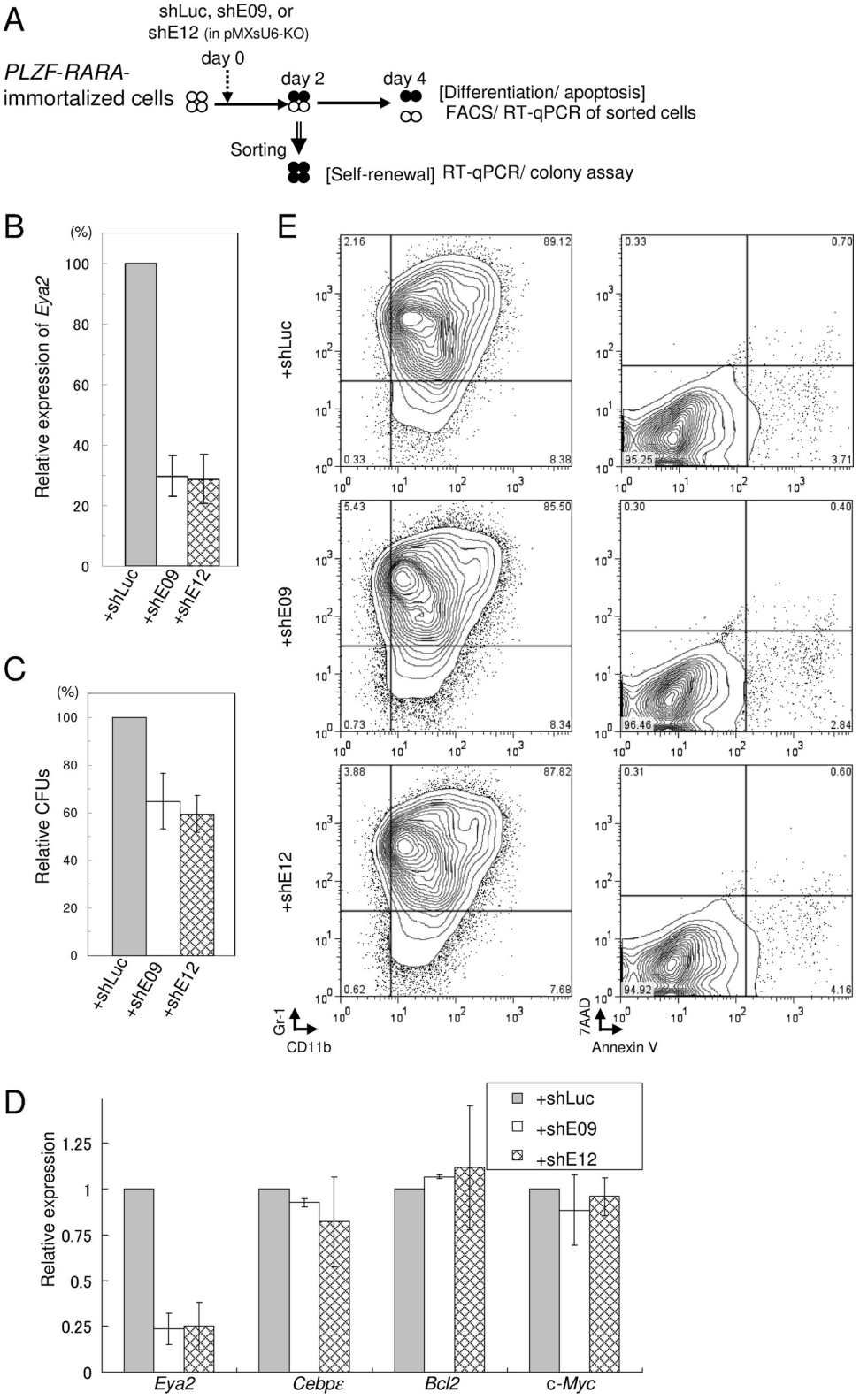

FIG 9 Reduced clonogenicity of *PLZF-RARA*-immortalized cells with *Eya2* depletion. (A) Experimental strategy for analysis of *PLZF-RARA*-immortalized cells with *Eya2* depletion by retroviral transduction of shRNA/*Kusabira-Orange* gene (*KO*) coexpressor in pMXsU6-KO. (B and C) Expression levels of *Eya2* by RT-qPCR (B) and relative CFU (3,000 cells/dish) (C) of the cells sorted from shRNA-transduced cells on day 2. (D and E) Expression levels of *Eya2*, *Cebpε*, *Bcl2*, and c-*Myc* by RT-qPCR (D) and immunophenotypes and apoptotic subpopulations by FACS analyses (E) of shRNA-transduced cells expressing KO on day 4. Bar graphs show means ± SD from three independent experiments.

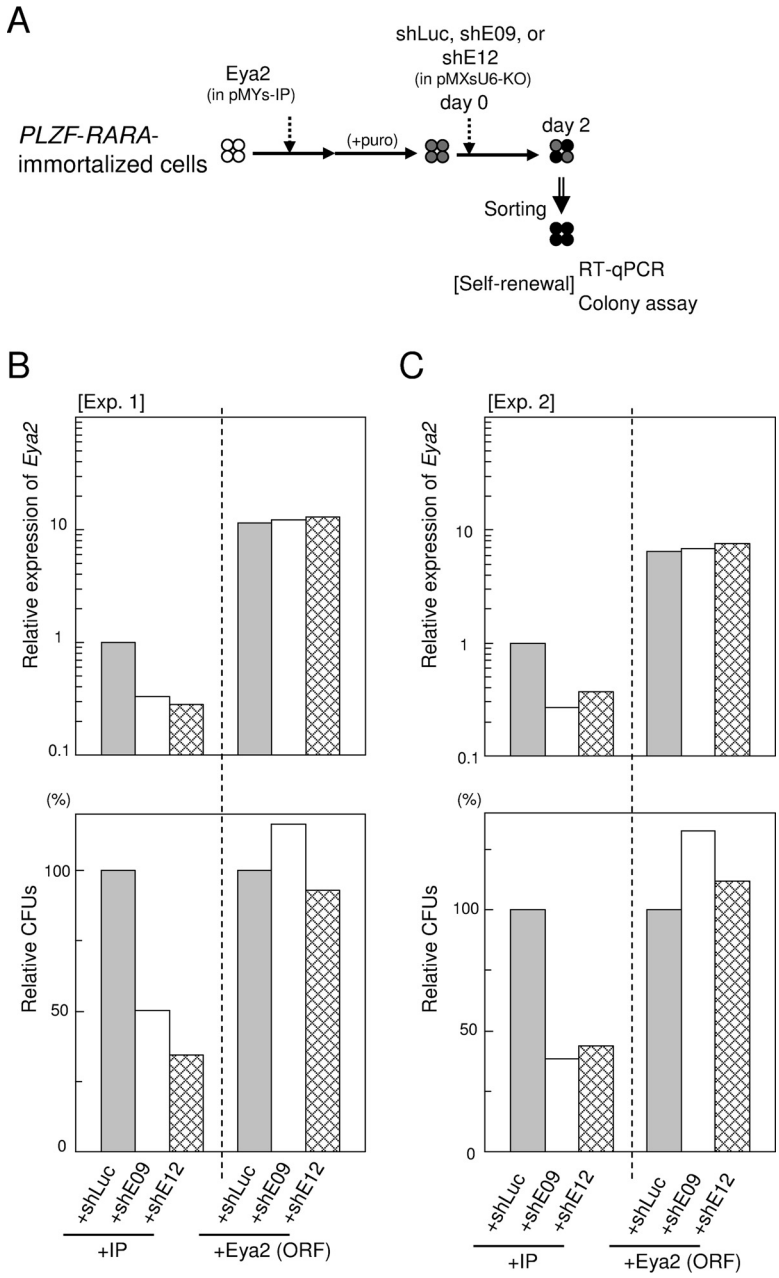

FIG 10 Restoration of clonogenicity of *PLZF-RARA*-immortalized cells with *Eya2* depletion by introduction of shRNA-resistant *Eya2*. (A) Experimental strategy for analysis of *PLZF-RARA*-immortalized cells forced to express shRNA-resistant *Eya2* with retroviral transduction of shRNA expressors. *PLZF-RARA*-immortalized cells were retrovirally transduced with the coding sequence alone of *Eya2* in pMYs-IP. Following puromycin (puro) selection for 3days, the immortalized cells force to express *Eya2* were next retrovirally transduced with shRNA expressors in pMXsU6-KO. (B and C) Expression levels of *Eya2* by RT-qPCR (upper panels) and relative CFU (3,000 cells/dish [bottom panels]) of the cells sorted from the shRNA-transduced cells on day 2.

DISCUSSION

The results of this study reveal a new key player, Eya2, in *PLZF-RARA*-mediated leukemic transformation, as well as in *Plzf*-mediated immortalization. A gain-of-function mutation of *Plzf* has been found to enable mouse BM cells to increase their self-renewal capacity (40), similarly to in our previous study (10), but the molecular mechanism is poorly understood. In the present study, we found induction of *Eya2* expression by transduction of *PLZF-RARA* and rapid and dose-dependent reduction of *Eya2* following

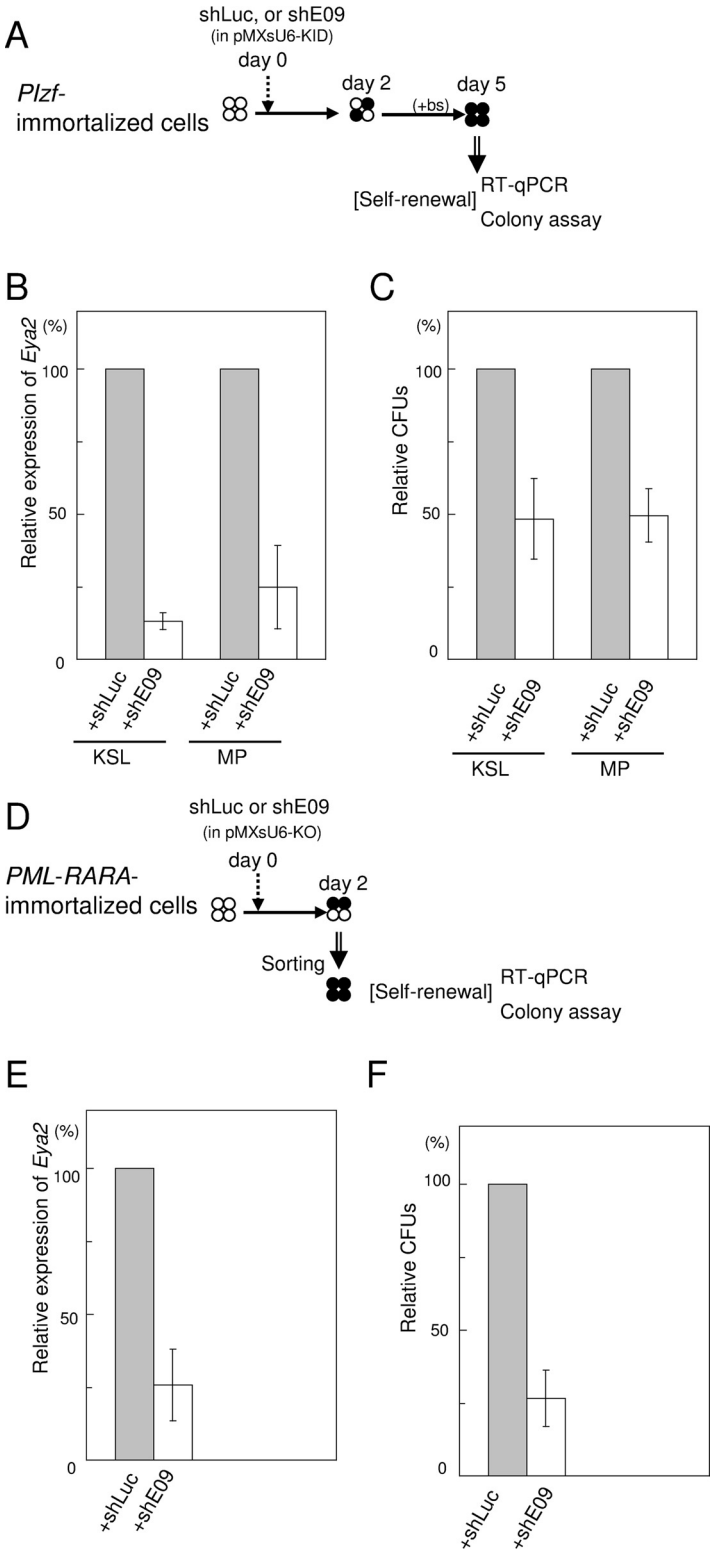

FIG 11 Reduced clonogenicity of *Plzf*-immortalized and *PML-RARA*-immortalized cells with *Eya2* depletion. (A) Experimental strategy for analysis of *Plzf*-immortalized cells using pMXsU6-KID. bs, blasticidin. (B and C) Expression levels of *Eya2* by RT-qPCR (B) and relative CFU (10,000 cells/dish) (C) of the shRNA-transduced cells. (D) Experimental strategy for analysis of *PML-RARA*-immortalized cells using pMXsU6-KO. (E and F) Expression levels of *Eya2* by RT-qPCR (E) and relative CFU (6,000 cells/dish) (F) of the sorted cells. Bar graphs show means ± SD from three independent experiments.

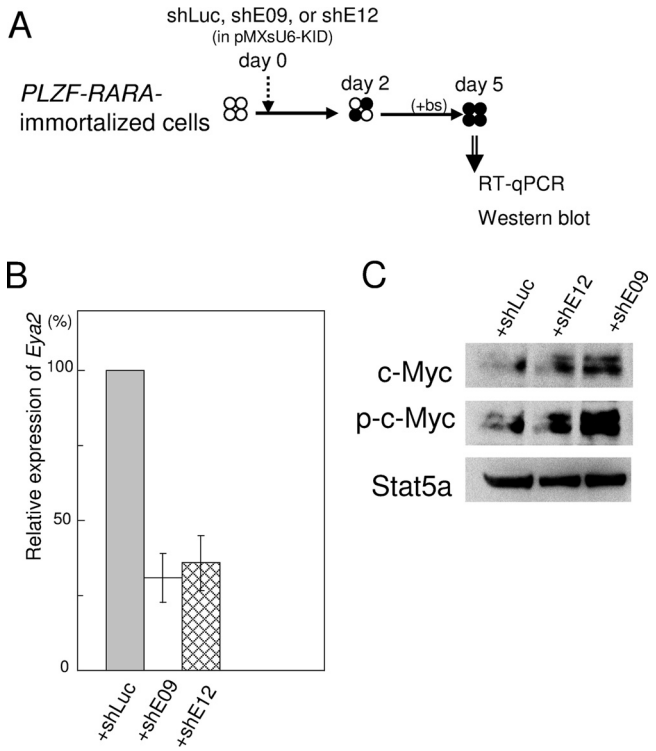

FIG 12 Possible regulation of c-Myc expression by Eya2 was not critically involved in *PLZF-RARA*-mediated immortalization. (A) Experimental strategy for analysis of *PLZF-RARA*-immortalized cells using pMXsU6-KID. bs, blasticidin. (B) Expression levels of *Eya2* by RT-qPCR in shRNA-transduced cells. (C) Expression levels of total c-Myc and Thr58-phosphorylated c-Myc by Western blotting analyses of *PLZF-RARA*-immortalized cells with *Eya2* depletion. Lysates extracted from the shRNA-transduced cells were blotted with anti-c-Myc (upper), anti-Thr58-phosphorylated c-Myc (p-c-Myc [middle]), and anti-Stat5a antibodies (bottom) as an internal control. Bar graphs show means ± SD from three independent experiments.

degradation of PLZF-RARA by ATRA, as well as upregulation of *Eya2* through promoter binding by Plzf. Higher expression of *Eya2* is also found in certain patients with *PLZF-RARA* APL (22) compared with patients with *PML-RARA* APL (34), although further analyses of more samples are needed. Meanwhile, high expression of some EMT-related genes is related to poor outcome in AML (41), which may partly explain a poor prognosis of *PLZF-RARA* APL in which EMT-associated *Eya2* is highly expressed. However, the reported common target genes of PLZF-RARA and PLZF include c-*Myc* and *DUSP6* (5, 20), but not *EYA2*. This discrepancy may be explained by differences in the cells or expression systems, including vectors, used in these studies. *EYA2* was also not identified as a target gene specific to *PLZF-RARA* in a previous study (42), whereas upregulation of c-*Myc* was found in human cord blood stem/progenitor cells retrovirally transduced with *PLZF* and in mouse hematopoietic stem/progenitor cells (HSPCs) retrovirally transduced with *PLZF-RARA* (5, 20), which resembles the pathway through Eya2 shared by *Plzf* and *PLZF-RARA* in the present study. Our findings implied that PLZF-RARA as a transcriptional activator is associated with aberrant self-renewal potential, whereas it is well known that PLZF-RARA as a transcriptional repressor induces differentiation block in leukemogenesis. Interestingly, GSEAs of human AML revealed that *EYA2* was highly expressed in a subtype of AML, including *PML-RARA* APL, which has human LSC- and mouse LT-HSC-associated features, compared with AML with low *EYA2* expression. Thus, induction of *Eya2* expression in *PML-RARA*-mediated immortalization of the mouse myeloid progenitor cells (Fig. 6C) might be associated with atypical *PML-RARA* APL with *EYA2* expression via unknown mechanisms.

Eya2 was capable of driving an aberrant self-renewal program on hematopoietic stem and/or progenitor cells *in vitro*, while bone marrow transplantation of retrovirally

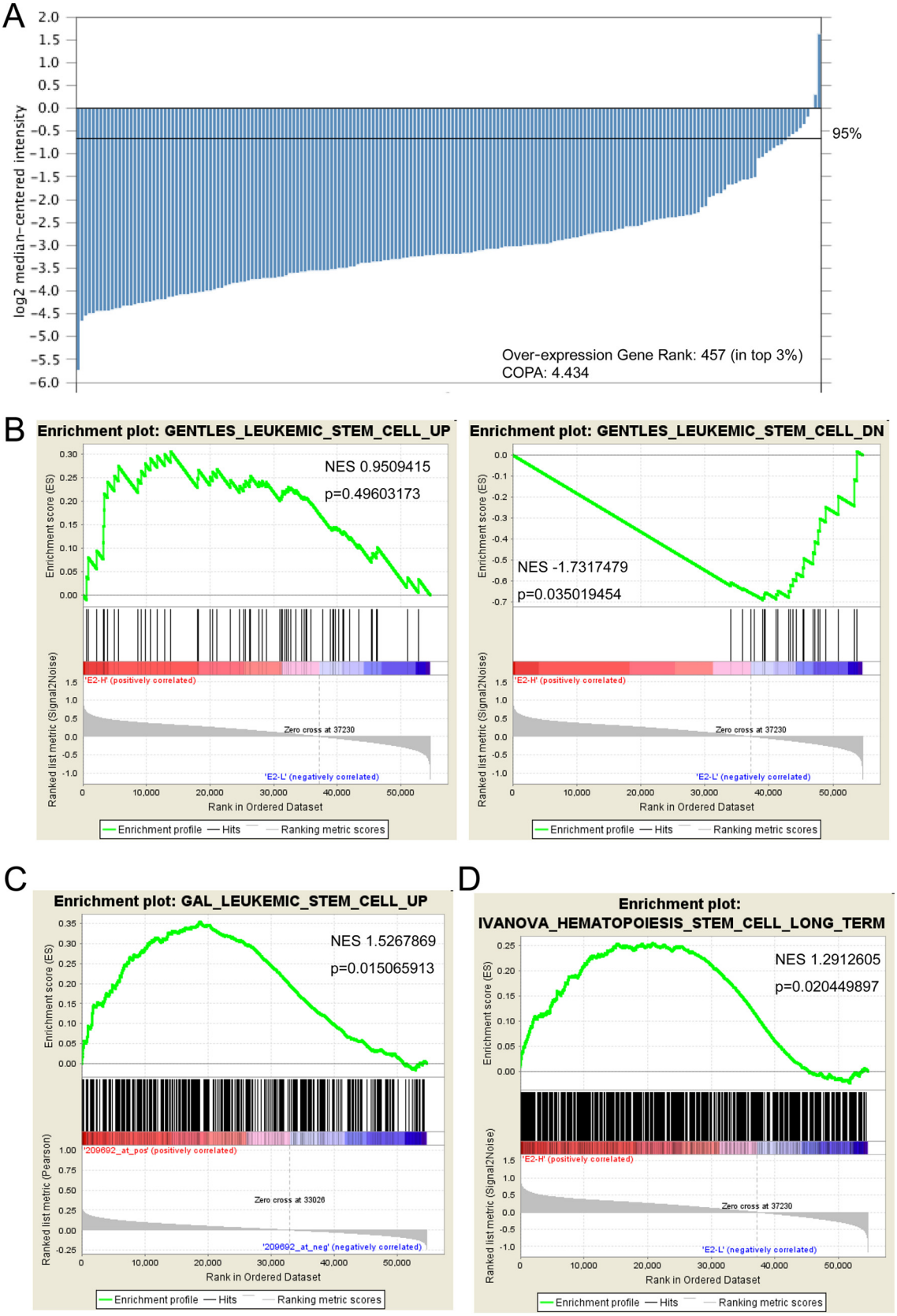

FIG 13 Characterization of a subtype of AML with high *EYA2* expression. (A) COPA revealing *EYA2* as a gene with an outlier profile at the 95th percentile in gene expression data for AML samples from TCGA. *EYA2* expression is shown in the waterfall plot using the Oncomine web platform. (B) GSEA of AML samples from TCGA showing that gene sets up- and downregulated in leukemic stem cells

(Continued on next page)

Eya2-transduced KSL cells did not lead to lethal hematological malignancy (data not shown), as in the case of *Plzf* in our previous work (10). This finding *in vitro* was in contrast to a previous study (43) showing induction of apoptosis by overexpression of *Eya2* in the mouse myeloid cell line 32D. This was reminiscent of similar contrasting results using *Plzf*-transduced 32D cells (44) compared with those using primary HSPCs in our study (10). In fly eye development (45), *Drosophila* Eya constitutes a regulatory network with the orthologue molecules Pax and Dach, which are also implicated in leukemogenesis (46, 47), as well as a critical partner, Six. Interestingly, one of the *Eya* family genes, *Eya1*, is highly expressed in mouse hematopoietic immature progenitor cells (48) and was recently reported to be a direct target gene of MLL-fusion protein as well as wild-type MLL (49). This is analogous to our findings of activation of *Eya2* by PLZF-RARA and PLZF. However, the roles of *Eya1* in *MLL*-fusion-mediated leukemogenesis and normal hematopoiesis remain unclear, although *Eya1* was found to immortalize mouse HSPCs in colony replating assays (49).

Our study of *Eya2* has unveiled several important properties, in addition to the immortalization potential of HSPCs. We found that *Eya2* can confer an aberrant self-renewal capacity on myeloid progenitor cells, without differentiation block. This finding implied that *Eya2* might be involved in the normal self-renewal potential of HSCs, because high *Eya2* expression occurs in LT-HSCs (30). In addition, we found that interaction of Eya2 with Six1 in the nucleus was required for the myeloid immortalization and that the full tyrosine phosphatase activity of Eya2 might be dispensable to the immortalization. However, we could not evaluate the phosphorylation level due to lack of identification of the appropriate target of the phosphatase in the immortalization. Therefore, further analysis of the requirement of the phosphatase activity is considered to be needed. It is noted that the phosphorylation level of a well-characterized target, histone H2AX, which is associated with cell survival and apoptosis, was not reduced by overexpression of *Eya2* in the myeloid immortalization assays (data not shown). Also, we did not examine the immortalization potential of Eya2 mutants that might reduce the phosphatase activity more severely and also affect the interaction with Six1: thus we cannot exclude the possibility that stronger inhibition of this activity would suppress *Eya2*-mediated immortalization.

Depletion of *Eya2* suppressed the clonogenicity of *PLZF-RARA*-immortalized myeloid progenitor cells and *Plzf*-immortalized hematopoietic stem and/or progenitor cells, without causing definite changes in the phenotypes for differentiation and apoptosis. This finding is consistent with findings that knockdown of EMT-related genes suppresses leukemogenesis (41). Surprisingly, *Eya2* depletion also reduced the clonogenicity of *PML-RARA*-immortalized myeloid progenitor cells. These results suggested that Eya2 may be a target of molecular therapy for a subtype of AML with high *EYA2* expression, irrespective of the phenotype. c-*Myc*, which is a critical target gene implicated in the ability of *PLZF-RARA*-immortalized HSPCs to survive and proliferate (20), was not affected by *Eya2* depletion in the immortalized myeloid cells. While shRNA-mediated reduction of c-*Myc* expression to about 40% of the control level leads to a 2-fold decrease in the clonogenicity of *PLZF-RARA*-immortalized HSPCs (20), conditional ablation of c-*Myc* in BM cells leads to severe cytopenia and accumulation of HSCs (50), which suggests that expression levels of c-*Myc* are not simply correlated to self-renewal capacity. Previous study (29) suggests that c-*Myc* is one of the target genes of Eya, despite there being no direct evidence of transcriptional regulation, and a recent study (36) showed stabilization of Myc via dephosphorylation by the

FIG 13 Legend (Continued)
(LSCs) (GENTLES_LEUKEMIC_STEM_CELL_UP and GENTLES_LEUKEMIC_STEM_CELL_DN) (37) were enriched insignificantly and significantly in clinical samples with high and low levels of *EYA2* expression, respectively. (C) GSEA of AML samples (GSE61804) showing that the gene set upregulated in leukemic stem cells (GAL_LEUKEMIC_STEM_CELL_UP) (38) was enriched in samples with high *EYA2* expression, compared with those with low expression, using continuous values of *EYA2* expression. (D) GSEA of AML samples from TCGA showing that the gene set upregulated in mouse LT-HSCs (IVANOVA_HEMATOPOIESIS_STEM_CELL_LONG_TERM) (39) was enriched in clinical samples expressing high levels of *EYA2*. NES, normalized enrichment score.

threonine phosphatase activity of Eya1. However, in *PLZF-RARA*-immortalized cells, neither the expression level of c-*Myc* transcripts nor that of c-Myc protein was affected by *Eya2* depletion. These results were compatible with our finding that ATRA treatment of *PLZF-RARA*-immortalized cells reduced expression of *Eya2* as rapidly as that of c-*Myc* (data not shown), thus suggesting that *Eya2* is largely not involved in upregulation and maintenance of c-Myc expression driven by *PLZF-RARA*. In line with this, the expression level of pT58-c-Myc was also not affected by Eya2. However, further biochemical characterization is needed to clarify the role of the threonine phosphatase activity of Eya2. Taken together, these results suggested that Eya2 plays an important role in the aberrant self-renewal potential induced by *PLZF-RARA*, but not through a mechanism involving c-*Myc*.

In conclusion, this study shows that a new key player, Eya2, was critically involved in *PLZF-RARA*-mediated leukemic transformation, as well as in *Plzf*-mediated immortalization. Also, *Eya2* was capable of driving an aberrant self-renewal program in hematopoietic stem and/or progenitor cells *in vitro*. An AML subtype with high *EYA2* expression was more closely associated with LSC gene expression signatures than other AMLs. Therefore, EYA2 may be a target for molecular therapy in this subtype of AML, which includes *PLZF-RARA* APL.

MATERIALS AND METHODS

Mice. All animal studies were approved by the Animal Care Committees of Mie University.

Reagents. 4-Hydroxytamoxifen (4OHT) and ATRA (Wako Pure Chemical Industries, Osaka, Japan) were dissolved in ethanol and used at a final concentration of 1 μM 4OHT and various concentrations of ATRA. For drug selection, G418 (Invitrogen, Carlsbad, CA), puromycin (Sigma-Aldrich, St. Louis, MO), and blasticidin S (Funakoshi, Tokyo, Japan) were used at final concentrations of 1 mg/ml, 1 μg/ml, and 20 μg/ml, respectively.

Retroviral constructs. The constructs harboring *Hoxa9*-internal ribosomal entry site (IRES)-*Meis1a*, *Plzf*, and *Plzf* mutant (*Plzf*$^{\Delta BTB}$) lacking its critical BTB/POZ (Broad-complex, Tramtrack, and bric à brac/poxvirus and zinc finger) domain were described previously (10, 51). A series of pMYs retroviral vectors (52) harboring a transgene were constructed by cloning the corresponding fragments as follows: fragments of coding regions of *Eya2*, *Eya2* ligated with a part of the 3′ untranslated region (UTR), and *Six1*, which were produced by reverse transcription (RT)-PCR of *Plzf*-immortalized KSL cells; fragments of mutants of *Eya2*, *Six1*, N-terminal FLAG-tagged *Eya2*, and N-terminal FLAG-tagged *Plzf*, which were produced by site-directed mutagenesis of the cloned *Eya2*, *Six1*, and *Plzf* genes; fragments of coding regions of the cloned *Plzf* (10) and *PLZF* (pF1KB6229) genes; a fragment of mouse estrogen receptor gene (*ER*)-*Eya2* fusion, which was produced by overlap extension PCR of the cloned *Eya2* and *ER*-fusion gene (10); and fragments of *RARA*-fusion genes, *PLZF* exons 1 to 3, or *PML* exons 1 to 6 fused with *RARA* exons 3 to 9, which were produced by overlap extension PCR of the cloned *PLZF* or *PML* (pF1KB4394) and *RARA* (pFN21AE1591 [Kazusa DNA Research Institute, Chiba, Japan]).

Purification of mouse hematopoietic stem and/or progenitor cells. Mouse hematopoietic stem and/or progenitor cells were purified as described previously (10) with modification. Bone marrow mononuclear cells (BMMNCs) were prepared from 8- to 12-week-old C57BL/6 mice. Using a magnetically activated cell sorting (MACS) cell separation system (Miltenyi Biotec, Auburn, CA), lineage (Lin)-depleted and Lin/Sca-1-depleted cells were isolated from BMMNCs, and the BMMNCs were labeled with biotinylated anti-Sca-1 antibody (E13-161.7 [Biolegend, San Diego, CA]) before magnetic purification, respectively. c-Kit$^+$ Sca-1$^+$ Lin$^-$ (KSL) and c-Kit$^+$ Sca-1$^-$ Lin$^-$ (enriched for myeloid progenitor [MP] cells) cells were purified from Lin-depleted cells using a FACSAria (BD Biosciences, Franklin Lakes, NJ).

Retroviral transduction. Retroviral supernatants of Plat E cells transfected with a retroviral construct were harvested 48 h after transfection (52). KSL, MP, Lin/Sca-1-depleted, and immortalized cells were transduced with retroviruses using RetroNectin (TaKaRa Bio, Inc., Otsu, Japan) as described previously (10).

Myeloid immortalization assay. Myeloid immortalization assays of retrovirally transduced cells using serial replating were performed as described previously (53). Briefly, every 5 to 7 days, colonies were enumerated, followed by replating of the harvested cells (0.5×10^4 to 1×10^4 cells/dish) in methylcellulose medium supplemented with 25 ng/ml mouse stem cell factor (SCF), and 10 ng/ml each of mouse interleukin-3 (IL-3), human IL-6, and mouse granulocyte-macrophage colony-stimulating factor (GM-CSF) (Miltenyi Biotec). The immortalized cells were harvested from colonies in the third plating and cultured in minimal essential medium alpha (α-MEM) supplemented with 20% fetal bovine serum (FBS) and the same cytokines.

To evaluate the effects of knockdown of *Eya2* and forced expression of Six1 or Six1 mutant in the immortalized cells, the *Eya2*-depleted or *Six1*/*Six1* mutant-transduced cells were plated in the same methylcellulose medium as that used in immortalization assays. Relative CFU were calculated as the percentage of the colony numbers compared with the corresponding controls (normalized to 100%) in each experiment after culture for 5 to 7 days.

TABLE 1 Sequences of primers used in this study

Primer type and gene or transcript	Primer sequence	
	Forward	Reverse
RT-qPCR (gene)		
Eya1	CCTTCTGGCGTCACAAGTCA	TTTAATGGGTGTGGAAGGACTGT
Eya2	TGTGCCTCAGCTCTTTGTGAA	GCTGTACTGTGTCTGGCCATAGG
Eya3	TGGTTAGGAACTGCGCTCAAGT	TGCGTGGTAGTGATCAGAACATT
Eya4	GAGGAAGAGGCCGGAAAAATAA	ATCCAAGTCCCAGACAAACACA
Six1	TGGAGCAGAAGGACCGAGTT	TGTCCAGCTCAGAAGAGGAGTTC
Cebpε	AAGGCCAAGAGGCGCATTAT	CGCTCGTTTTCAGCCATGTAC
Bcl2	CATCTGCACACCTGGATCCA	ATCAAACAGAGGTCGCATGCT
c-*Myc*	AGCCCCTAGTGCTGCATGAG	CCACAGACACCACATCAATTTCTT
Actb	AGAGGGAAATCGTGCGTGAC	CAATAGTGATGACCTGGCCGT
PLZF	GAAGTCAGAGAGCCGGACCAT	GCTCGCACCCGTACGTCTT
ChIP-qPCR (gene)		
Hbb-b1	GCTTCTGACATAGTTGTGTTGACTCA	CAGCAGCCTTCTCAGCATCA
$Eya2_a$	GCAGCCCTGCGACATTC	ACCCGCACAGTGCAGAGTC
$Eya2_b$	TGGGAGGTAGAAAGGCTATCCTT	TCTCAGTCAGTACACAGTGACATCCA
$Eya2_{c\text{-}1}$	AGGACCAGGTGATGGATCAGAT	GGGACAGGTGCTCACATAGAAAG
$Eya2_{c\text{-}2}$	GCAGAAGAAGCAGTGGTTTCTAACA	CCACGGTCAAGGACTTAAACACA
$Eya2_{c\text{-}3}$	GCACACCTGTGACACGTACACA	GGAAAGGTAGAGAGAGAGGGAGTGTAAT
$Eya2_{c\text{-}4}$	CTCACAAACCACAAAACTCACCAT	GGCAGCTTGTGAGTCATTCCTA
RT-PCR (transcript)		
$Eya2_{\text{exons 1a-4}}$	TCGGGACGACTCTGCACTGT	GCTGTACTGTGTCTGGCCATAGG
$Eya2_{\text{exons 1b-4}}$	GTAAGGTCCCATGGACCCCA	GCTGTACTGTGTCTGGCCATAGG
$Eya2_{\text{exons 1c-4}}$	GGAGCTAGAACAAGCAGCAGGAAA	GCTGTACTGTGTCTGGCCATAGG

FACS analysis. Immunophenotypical analyses and apoptosis detection were performed using a FACSCalibur (BD Biosciences) as described previously (10). Data were analyzed with FlowJo (Tree Star, Ashland, OR).

Gene silencing. The target sequences against the *Eya2* and *luciferase* genes were 5′-GTGTTTCAGA GACAATCAT-3′ (shE09) and 5′-GCCTTATGCCGCCATCTTG-3′ (shE12), and the same sequence (shLuc) described previously (10), respectively. As a loop sequence, 5′-CTTCAAGAGAG-3′ was used (54). Short hairpin RNA (shRNA) sequences against *Eya2* or *luciferase* were inserted into pMXsU6-KO (10) or pMXsU6-KID, where an IRES cassette derived from pMYs-IG ligated with the *blasticidin S deaminase* gene (a kind gift from M. Kimura) was inserted just after the *Kusabira-Orange* (*KO*) gene in pMXsU6-KO. Cells transduced with pMXsU6-KO, or pMXsU6-KID were subjected to sorting by KO expression on the FACSAria or blasticidin selection starting 2 days after transduction.

ChIP. ChIP was performed as described previously (10). Briefly, the chromatin prepared from FLAG-tagged-*Plzf*-immortalized cells was precipitated using Dynabeads anti-mouse IgG (Invitrogen) preincubated with mouse monoclonal anti-FLAG (M2; Sigma-Aldrich), mouse monoclonal anti-RNA polymerase II (CTD4H8; Millipore, Temecula, CA), or mouse IgG1 antibody (Biolegend). Precipitated complexes were purified and subjected to quantitative PCR (qPCR).

RT of RNA. RNA extraction and RT were performed using TRI Reagent LS (Molecular Research Center, Inc., Cincinnati, OH) and SuperScript II (Invitrogen) with random hexamers, respectively, as described previously (10).

PCR. Quantitative PCR (qPCR) analyses were performed using KOD SYBR qPCR mix (for ChIP products; Toyobo, Osaka, Japan) or PowerSYBR green PCR master mix (for cDNA) on a StepOnePlus real-time PCR system (Applied Biosystems, Foster City, CA) (10). For RT-qPCR, after quantification of the expression levels of samples using the threshold cycle ($2^{-\Delta\Delta CT}$) method and normalization relative to *B2m* (default), *Actb*, or *PLZF*, the relative expression levels were calculated. For ChIP-qPCR, after C_T values of ChIP products were measured and normalized with those of corresponding input samples using the $2^{-\Delta\Delta CT}$ method, the percentages of samples relative to input were calculated. Primer sets for ChIP-qPCR were designed around the regions just upstream of three distinct putative transcription start sites (TSSs) of *Eya2* on the basis of NCBI reference sequences (NM_001271963.1 [exon 1a], NM_001271962.1 [exon 1b], and NM_010165.3 [exon 1c]). The promoter region of *Hbb-b1* was used as a negative control. To detect the transcripts of *Eya2* and *B2m* by RT-PCR, PCR amplifications of cDNA were run for 32 and 26 cycles (94°C for 30 s, 55°C for 30 s, and 68°C for 30 s), respectively, using Quick *Taq* HS DyeMix (Toyobo). The sequences of the primers used are listed in Table 1, except for those for *B2m* (10).

Immunoprecipitation and Western blot analysis. Expression of transgenes in transfected cells was examined by Western blotting analyses, as described previously (55) with modification. Briefly, the transfected cells were harvested with lysis buffer (50 mM Tris-HCl [pH 7.5], 150 mM NaCl, 1 mM EDTA [pH 8.0], 1% Nonidet P-40) supplemented with protease inhibitor cocktail (Sigma-Aldrich) and 2 mM phenylmethylsulfonyl fluoride. Lysates from cells transfected with pMYs-PML-RARA-IN were subjected to immunoprecipitation with rabbit polyclonal anti-RARA antibody (C-20; Santa Cruz Biotechnology, Dallas, TX) as described previously (53). The other lysates were mixed with an equal volume of 2× SDS sample buffer. Retrovirally transduced KSL cells, *Eya2*-immortalized KSL cells, and *PLZF-RARA*-immortalized cells

with ATRA treatment or *Eya2* depletion were directly lysed in 1× SDS sample buffer, followed by sonication. The prepared samples were boiled, followed by Western blotting analyses using rabbit polyclonal anti-Eya2 (ab116075; Abcam, Cambridge, United Kingdom), anti-RARA, anti-ERα (anti-ER, MC-20), anti-STAT5a (L-20), anti-p-c-Myc (Thr58), goat polyclonal anti-Six1 (A-20), mouse monoclonal anti-c-Myc (C-33), anti-PLZF (D9, Santa Cruz Biotechnology), anti-FLAG, and anti-α-tubulin (Sigma-Aldrich) antibodies.

Immunostaining. Immunostaining of the immortalized cells was performed as described previously (56) with modification. Briefly, cytospin preparations of the cells were fixed with phosphate-buffered 4% paraformaldehyde and treated with 0.1% Triton X-100 (Wako Pure Chemical Industries) in PBS. The preparations were reacted with rabbit polyclonal anti-DDDDK-tag (PM020; MBL, Nagoya, Japan) or anti-ER antibodies, stained with Alexa Fluor 568-conjugated goat anti-rabbit IgG secondary antibody and TO-PRO-3 iodide (Molecular Probe, Thermo Fisher Scientific, Waltham, MA), and viewed with IX81 FV1000 confocal microscope (Olympus, Tokyo, Japan).

Statistical analysis. Comparisons of bar charts were performed by *t* test.

Bioinformatics analysis. Genetic information on the genomic region covering *Eya2* and its upstream sequence in the mouse were obtained from the University of California, Santa Cruz (UCSC) Genomic Browser (http://genome.ucsc.edu/). ChIP-seq data in the same region were also obtained from ENCODE/LICR (Ren Laboratory, Ludwig Institute for Cancer Research, the University of California, San Diego) through the UCSC Genome Browser.

Gene expression profiling data deposited in the Gene Expression Omnibus (GEO) were analyzed with 5 *PLZF-RARA* APL samples from GSE8510 (22) and 15 *PML-RARA* APL samples from GSE61804 (34) for human *RARA*-rearranged leukemia samples. Probe intensities in CEL data files were summarized and normalized by MAS5.0, followed by quantile normalization, using the statistical programming language R (http://www.r-project.org). Expression levels of *EYA2* and *ACTB* were compared based on intensities using probes 209692_at and 200801_x_at (Affymetrix, Santa Clara, CA), respectively. Gene expression profiling data of 105 AML samples, including 13 t(15;17) APL samples in GSE12662 (1 APL sample was not used due to an ambiguous status of chromosomal translocation) (35), were obtained from GEO and subjected to cancer outlier profile analysis (COPA) transformation (57). COPAs were also performed for The Cancer Genome Atlas (TCGA) (http://cancergenome.nih.gov/) AML expression data set of 197 AML samples, including 20 APL samples in the Oncomine 4.5 (http://www.oncomine.org) database and data-mining platform. Expression values using the 209692_at probe for detection of *EYA2* were used to subdivide the AML samples into $EYA2^{high}$ (TCGA-AB-2920-03A-01R-0757-21, TCGA-AB-2843-03A-01R-0757-21, TCGA-AB-2830-03A-01R-0757-21, TCGA-AB-2935-03A-01R-0757-21, TCGA-AB-2857-03A-01R-0757-21, TCGA-AB-2848-03A-01R-0757-21, TCGA-AB-3012-03A-01R-0757-21, TCGA-AB-2895-03A-01R-0757-21, and TCGA-AB-2949-03B-01R-0757-21) and $EYA2^{low}$ (TCGA-AB-2886-03A-01R-0757-21, TCGA-AB-2845-03B-01R-0757-21, TCGA-AB-2831-03A-01R-0757-21, TCGA-AB-2956-03A-01R-0757-21, TCGA-AB-2853-03A-01R-0757-21, TCGA-AB-2922-03A-01R-0757-21, TCGA-AB-3007-03A-01R-0757-21, TCGA-AB-2982-03B-01R-0757-21, and TCGA-AB-2986-03A-01R-0757-21) subgroups. Gene set enrichment analyses (GSEAs) were performed using GSEA version 2.2.2 software (Broad Institute (http://www.broadinstitute.org/gsea)) with Signal2Noise or Pearson metrics for gene ranking and 1,000 data permutations. Gene sets were downloaded from the Molecular Signatures Database (http://www.broadinstitute.org/gsea/msigdb/index.jsp).

Accession number(s). cDNA microarray data in the present study have been deposited in the GEO database under accession no. GSE84771.

ACKNOWLEDGMENTS

We thank Makoto Kimura for a plasmid harboring the *blasticidin S deaminase* gene, the TCGA Research Network for providing data, and Palabra, Inc. (Kyoto, Japan), for language assistance.

R.O. and T.N. designed the research. R.O., M.M., and S.I. performed experiments. R.O., N.K., and T.N. analyzed the results. R.O. and T.N. wrote the manuscript.

This study was supported by Grants-in-Aid from the Ministry of Education, Culture, Sports, Science, and Technology in Japan (T.N.; Basic-B; 26293247), the Foundation for Promotion of Cancer Research (R.O.), Sanikai (R.O.), the Japan Leukemia Research Fund (T.N.), Okasan-Kato Foundation (T.N.), and the Mie University Hospital Seed Grant Program (T.N.).

The funders had no role in study design, data collection and interpretation, or the decision to submit the work for publication.

We declare we have no competing financial interests.

REFERENCES

1. Visvader JE. 2011. Cells of origin in cancer. Nature 469:314–322. https://doi.org/10.1038/nature09781.
2. Kreso A, Dick JE. 2014. Evolution of the cancer stem cell model. Cell Stem Cell 14:275–291. https://doi.org/10.1016/j.stem.2014.02.006.
3. Rosenbauer F, Tenen DG. 2007. Transcription factors in myeloid development: balancing differentiation with transformation. Nat Rev Immunol 7:105–117. https://doi.org/10.1038/nri2024.
4. Kitamura T, Watanabe-Okochi N, Enomoto Y, Nakahara F, Oki T, Komeno

Y, Kato N, Doki N, Uchida T, Kagiyama Y, Togami K, Kawabata KC, Nishimura K, Hayashi Y, Nagase R, Saika M, Fukushima T, Asada S, Fujino T, Izawa Y, Horikawa S, Fukuyama T, Tanaka Y, Ono R, Goyama S, Nosaka T, Kitaura J, Inoue D. 2016. Novel working hypothesis for pathogenesis of hematological malignancies: combination of mutations-induced cellular phenotypes determines the disease (cMIP-DD). J Biochem 159:17–25. https://doi.org/10.1093/jb/mvv114.

5. Doulatov S, Notta F, Rice KL, Howell L, Zelent A, Licht JD, Dick JE. 2009. PLZF is a regulator of homeostatic and cytokine-induced myeloid development. Genes Dev 23:2076–2087. https://doi.org/10.1101/gad.1788109.
6. Barna M, Merghoub T, Costoya JA, Ruggero D, Branford M, Bergia A, Samori B, Pandolfi PP. 2002. Plzf mediates transcriptional repression of *HoxD* gene expression through chromatin remodeling. Dev Cell 3:499–510. https://doi.org/10.1016/S1534-5807(02)00289-7.
7. Reid A, Gould A, Brand N, Cook M, Strutt P, Li J, Licht J, Waxman S, Krumlauf R, Zelent A. 1995. Leukemia translocation gene, *PLZF*, is expressed with a speckled nuclear pattern in early hematopoietic progenitors. Blood 86:4544–4552.
8. Liu TM, Lee EH, Lim B, Shyh-Chang N. 2016. Concise review: balancing stem cell self-renewal and differentiation with PLZF. Stem Cells 34:277–287. https://doi.org/10.1002/stem.2270.
9. Vincent-Fabert C, Platet N, Vandevelde A, Poplineau M, Koubi M, Finetti P, Tiberi G, Imbert AM, Bertucci F, Duprez E. 2016. PLZF mutation alters mouse hematopoietic stem cell function and cell cycle progression. Blood 127:1881–1885. https://doi.org/10.1182/blood-2015-09-666974.
10. Ono R, Masuya M, Nakajima H, Enomoto Y, Miyata E, Nakamura A, Ishii S, Suzuki K, Shibata-Minoshima F, Katayama N, Kitamura T, Nosaka T. 2013. Plzf drives *MLL*-fusion-mediated leukemogenesis specifically in long-term hematopoietic stem cells. Blood 122:1271–1283. https://doi.org/10.1182/blood-2012-09-456665.
11. Chen SJ, Zelent A, Tong JH, Yu HQ, Wang ZY, Derre J, Berger R, Waxman S, Chen Z. 1993. Rearrangements of the retinoic acid receptor alpha and promyelocytic leukemia zinc finger genes resulting from t(11;17)(q23;q21) in a patient with acute promyelocytic leukemia. J Clin Invest 91:2260–2267. https://doi.org/10.1172/JCI116453.
12. He LZ, Merghoub T, Pandolfi PP. 1999. In vivo analysis of the molecular pathogenesis of acute promyelocytic leukemia in the mouse and its therapeutic implications. Oncogene 18:5278–5292. https://doi.org/10.1038/sj.onc.1203088.
13. Zelent A, Guidez F, Melnick A, Waxman S, Licht JD. 2001. Translocations of the *RARα* gene in acute promyelocytic leukemia. Oncogene 20:7186–7203. https://doi.org/10.1038/sj.onc.1204766.
14. Zeisig BB, Kwok C, Zelent A, Shankaranarayanan P, Gronemeyer H, Dong S, So CW. 2007. Recruitment of RXR by homotetrameric RARα fusion proteins is essential for transformation. Cancer Cell 12:36–51. https://doi.org/10.1016/j.ccr.2007.06.006.
15. Ablain J, de Thé H. 2011. Revisiting the differentiation paradigm in acute promyelocytic leukemia. Blood 117:5795–5802. https://doi.org/10.1182/blood-2011-02-329367.
16. de Thé H, Chen Z. 2010. Acute promyelocytic leukaemia: novel insights into the mechanisms of cure. Nat Rev Cancer 10:775–783. https://doi.org/10.1038/nrc2943.
17. Dos Santos GA, Kats L, Pandolfi PP. 2013. Synergy against PML-RARa: targeting transcription, proteolysis, differentiation, and self-renewal in acute promyelocytic leukemia. J Exp Med 210:2793–2802. https://doi.org/10.1084/jem.20131121.
18. Rego EM, Ruggero D, Tribioli C, Cattoretti G, Kogan S, Redner RL, Pandolfi PP. 2006. Leukemia with distinct phenotypes in transgenic mice expressing PML/RARα, PLZF/RARα or NPM/RARα. Oncogene 25:1974–1979. https://doi.org/10.1038/sj.onc.1209216.
19. Boukarabila H, Saurin AJ, Batsche E, Mossadegh N, van Lohuizen M, Otte AP, Pradel J, Muchardt C, Sieweke M, Duprez E. 2009. The PRC1 Polycomb group complex interacts with PLZF/RARA to mediate leukemic transformation. Genes Dev 23:1195–1206. https://doi.org/10.1101/gad.512009.
20. Rice KL, Hormaeche I, Doulatov S, Flatow JM, Grimwade D, Mills KI, Leiva M, Ablain J, Ambardekar C, McConnell MJ, Dick JE, Licht JD. 2009. Comprehensive genomic screens identify a role for PLZF-RARα as a positive regulator of cell proliferation via direct regulation of c-MYC. Blood 114:5499–5511. https://doi.org/10.1182/blood-2009-03-206524.
21. He LZ, Bhaumik M, Tribioli C, Rego EM, Ivins S, Zelent A, Pandolfi PP. 2000. Two critical hits for promyelocytic leukemia. Mol Cell 6:1131–1141. https://doi.org/10.1016/S1097-2765(00)00111-8.
22. Guidez F, Parks S, Wong H, Jovanovic JV, Mays A, Gilkes AF, Mills KI, Guillemin MC, Hobbs RM, Pandolfi PP, de The H, Solomon E, Grimwade D. 2007. RARα-PLZF overcomes PLZF-mediated repression of *CRABPI*, contributing to retinoid resistance in t(11;17) acute promyelocytic leukemia. Proc Natl Acad Sci U S A 104:18694–18699. https://doi.org/10.1073/pnas.0704433104.
23. Bonini NM, Leiserson WM, Benzer S. 1993. The *eyes absent* gene: genetic control of cell survival and differentiation in the developing Drosophila eye. Cell 72:379–395. https://doi.org/10.1016/0092-8674(93)90115-7.
24. Jemc J, Rebay I. 2007. The eyes absent family of phosphotyrosine phosphatases: properties and roles in developmental regulation of transcription. Annu Rev Biochem 76:513–538. https://doi.org/10.1146/annurev.biochem.76.052705.164916.
25. Cook PJ, Ju BG, Telese F, Wang X, Glass CK, Rosenfeld MG. 2009. Tyrosine dephosphorylation of H2AX modulates apoptosis and survival decisions. Nature 458:591–596. https://doi.org/10.1038/nature07849.
26. Krishnan N, Jeong DG, Jung SK, Ryu SE, Xiao A, Allis CD, Kim SJ, Tonks NK. 2009. Dephosphorylation of the C-terminal tyrosyl residue of the DNA damage-related histone H2A.X is mediated by the protein phosphatase eyes absent. J Biol Chem 284:16066–16070. https://doi.org/10.1074/jbc.C900032200.
27. Okabe Y, Sano T, Nagata S. 2009. Regulation of the innate immune response by threonine-phosphatase of Eyes absent. Nature 460:520–524. https://doi.org/10.1038/nature08138.
28. Ohto H, Kamada S, Tago K, Tominaga SI, Ozaki H, Sato S, Kawakami K. 1999. Cooperation of six and eya in activation of their target genes through nuclear translocation of Eya. Mol Cell Biol 19:6815–6824. https://doi.org/10.1128/MCB.19.10.6815.
29. Li X, Oghi KA, Zhang J, Krones A, Bush KT, Glass CK, Nigam SK, Aggarwal AK, Maas R, Rose DW, Rosenfeld MG. 2003. Eya protein phosphatase activity regulates Six1-Dach-Eya transcriptional effects in mammalian organogenesis. Nature 426:247–254. https://doi.org/10.1038/nature02083.
30. Forsberg EC, Prohaska SS, Katzman S, Heffner GC, Stuart JM, Weissman IL. 2005. Differential expression of novel potential regulators in hematopoietic stem cells. PLoS Genet 1:e28. https://doi.org/10.1371/journal.pgen.0010028.
31. Zhang L, Yang N, Huang J, Buckanovich RJ, Liang S, Barchetti A, Vezzani C, O'Brien-Jenkins A, Wang J, Ward MR, Courreges MC, Fracchioli S, Medina A, Katsaros D, Weber BL, Coukos G. 2005. Transcriptional coactivator Drosophila *Eyes Absent Homologue 2* is up-regulated in epithelial ovarian cancer and promotes tumor growth. Cancer Res 65:925–932.
32. Farabaugh SM, Micalizzi DS, Jedlicka P, Zhao R, Ford HL. 2012. Eya2 is required to mediate the pro-metastatic functions of Six1 via the induction of TGF-beta signaling, epithelial-mesenchymal transition, and cancer stem cell properties. Oncogene 31:552–562. https://doi.org/10.1038/onc.2011.259.
33. Patrick AN, Cabrera JH, Smith AL, Chen XS, Ford HL, Zhao R. 2013. Structure-function analyses of the human SIX1-EYA2 complex reveal insights into metastasis and BOR syndrome. Nat Struct Mol Biol 20:447–453. https://doi.org/10.1038/nsmb.2505.
34. Metzelder SK, Michel C, von Bonin M, Rehberger M, Hessmann E, Inselmann S, Solovey M, Wang Y, Sohlbach K, Brendel C, Stiewe T, Charles J, Ten Haaf A, Ellenrieder V, Neubauer A, Gattenlohner S, Bornhauser M, Burchert A. 2015. NFATc1 as a therapeutic target in FLT3-ITD-positive AML. Leukemia 29:1470–1477. https://doi.org/10.1038/leu.2015.95.
35. Payton JE, Grieselhuber NR, Chang LW, Murakami M, Geiss GK, Link DC, Nagarajan R, Watson MA, Ley TJ. 2009. High throughput digital quantification of mRNA abundance in primary human acute myeloid leukemia samples. J Clin Invest 119:1714–1726. https://doi.org/10.1172/JCI38248.
36. Xu J, Wong EY, Cheng C, Li J, Sharkar MT, Xu CY, Chen B, Sun J, Jing D, Xu PX. 2014. Eya1 interacts with Six2 and Myc to regulate expansion of the nephron progenitor pool during nephrogenesis. Dev Cell 31:434–447. https://doi.org/10.1016/j.devcel.2014.10.015.
37. Gentles AJ, Plevritis SK, Majeti R, Alizadeh AA. 2010. Association of a leukemic stem cell gene expression signature with clinical outcomes in acute myeloid leukemia. JAMA 304:2706–2715. https://doi.org/10.1001/jama.2010.1862.
38. Gal H, Amariglio N, Trakhtenbrot L, Jacob-Hirsh J, Margalit O, Avigdor A, Nagler A, Tavor S, Ein-Dor L, Lapidot T, Domany E, Rechavi G, Givol D. 2006. Gene expression profiles of AML derived stem cells; similarity to hematopoietic stem cells. Leukemia 20:2147–2154. https://doi.org/10.1038/sj.leu.2404401.
39. Ivanova NB, Dimos JT, Schaniel C, Hackney JA, Moore KA, Lemischka IR.

2002. A stem cell molecular signature. Science 298:601–604. https://doi.org/10.1126/science.1073823.
40. Puszyk W, Down T, Grimwade D, Chomienne C, Oakey RJ, Solomon E, Guidez F. 2013. The epigenetic regulator PLZF represses L1 retrotransposition in germ and progenitor cells. EMBO J 32:1941–1952. https://doi.org/10.1038/emboj.2013.118.
41. Stavropoulou V, Kaspar S, Brault L, Sanders MA, Juge S, Morettini S, Tzankov A, Iacovino M, Lau IJ, Milne TA, Royo H, Kyba M, Valk PJ, Peters AH, Schwaller J. 2016. MLL-AF9 expression in hematopoietic stem cells drives a highly invasive AML expressing EMT-related genes linked to poor outcome. Cancer Cell 30:43–58. https://doi.org/10.1016/j.ccell.2016.05.011.
42. Spicuglia S, Vincent-Fabert C, Benoukraf T, Tiberi G, Saurin AJ, Zacarias-Cabeza J, Grimwade D, Mills K, Calmels B, Bertucci F, Sieweke M, Ferrier P, Duprez E. 2011. Characterisation of genome-wide PLZF/RARA target genes. PLoS One 6:e24176. https://doi.org/10.1371/journal.pone.0024176.
43. Clark SW, Fee BE, Cleveland JL. 2002. Misexpression of the *Eyes Absent* family triggers the apoptotic program. J Biol Chem 277:3560–3567. https://doi.org/10.1074/jbc.M108410200.
44. Shaknovich R, Yeyati PL, Ivins S, Melnick A, Lempert C, Waxman S, Zelent A, Licht JD. 1998. The promyelocytic leukemia zinc finger protein affects myeloid cell growth, differentiation, and apoptosis. Mol Cell Biol 18:5533–5545. https://doi.org/10.1128/MCB.18.9.5533.
45. Wagner GP. 2007. The developmental genetics of homology. Nat Rev Genet 8:473–479. https://doi.org/10.1038/nrg2099.
46. Mullighan CG, Goorha S, Radtke I, Miller CB, Coustan-Smith E, Dalton JD, Girtman K, Mathew S, Ma J, Pounds SB, Su X, Pui CH, Relling MV, Evans WE, Shurtleff SA, Downing JR. 2007. Genome-wide analysis of genetic alterations in acute lymphoblastic leukaemia. Nature 446:758–764. https://doi.org/10.1038/nature05690.
47. Nebral K, Denk D, Attarbaschi A, Konig M, Mann G, Haas OA, Strehl S. 2009. Incidence and diversity of *PAX5* fusion genes in childhood acute lymphoblastic leukemia. Leukemia 23:134–143. https://doi.org/10.1038/leu.2008.306.
48. Terskikh AV, Miyamoto T, Chang C, Diatchenko L, Weissman IL. 2003. Gene expression analysis of purified hematopoietic stem cells and committed progenitors. Blood 102:94–101. https://doi.org/10.1182/blood-2002-08-2509.
49. Wang QF, Wu G, Mi S, He F, Wu J, Dong J, Luo RT, Mattison R, Kaberlein JJ, Prabhakar S, Ji H, Thirman MJ. 2011. MLL fusion proteins preferentially regulate a subset of wild-type MLL target genes in the leukemic genome. Blood 117:6895–6905. https://doi.org/10.1182/blood-2010-12-324699.
50. Wilson A, Murphy MJ, Oskarsson T, Kaloulis K, Bettess MD, Oser GM, Pasche AC, Knabenhans C, Macdonald HR, Trumpp A. 2004. c-Myc controls the balance between hematopoietic stem cell self-renewal and differentiation. Genes Dev 18:2747–2763. https://doi.org/10.1101/gad.313104.
51. Ono R, Kumagai H, Nakajima H, Hishiya A, Taki T, Horikawa K, Takatsu K, Satoh T, Hayashi Y, Kitamura T, Nosaka T. 2009. Mixed-lineage-leukemia (MLL) fusion protein collaborates with Ras to induce acute leukemia through aberrant *Hox* expression and Raf activation. Leukemia 23:2197–2209. https://doi.org/10.1038/leu.2009.177.
52. Kitamura T, Koshino Y, Shibata F, Oki T, Nakajima H, Nosaka T, Kumagai H. 2003. Retrovirus-mediated gene transfer and expression cloning: powerful tools in functional genomics. Exp Hematol 31:1007–1014. https://doi.org/10.1016/S0301-472X(03)00260-1.
53. Ono R, Nakajima H, Ozaki K, Kumagai H, Kawashima T, Taki T, Kitamura T, Hayashi Y, Nosaka T. 2005. Dimerization of MLL fusion proteins and FLT3 activation synergize to induce multiple-lineage leukemogenesis. J Clin Invest 115:919–929. https://doi.org/10.1172/JCI200522725.
54. Gu S, Jin L, Zhang Y, Huang Y, Zhang F, Valdmanis PN, Kay MA. 2012. The loop position of shRNAs and pre-miRNAs is critical for the accuracy of dicer processing in vivo. Cell 151:900–911. https://doi.org/10.1016/j.cell.2012.09.042.
55. Ono R, Ihara M, Nakajima H, Ozaki K, Kataoka-Fujiwara Y, Taki T, Nagata K, Inagaki M, Yoshida N, Kitamura T, Hayashi Y, Kinoshita M, Nosaka T. 2005. Disruption of *Sept6*, a fusion partner gene of *MLL*, does not affect ontogeny, leukemogenesis induced by *MLL-SEPT6*, or phenotype induced by the loss of *Sept4*. Mol Cell Biol 25:10965–10978. https://doi.org/10.1128/MCB.25.24.10965-10978.2005.
56. Miyata E, Masuya M, Yoshida S, Nakamura S, Kato K, Sugimoto Y, Shibasaki T, Yamamura K, Ohishi K, Nishii K, Ishikawa F, Shiku H, Katayama N. 2008. Hematopoietic origin of hepatic stellate cells in the adult liver. Blood 111:2427–2435. https://doi.org/10.1182/blood-2007-07-101261.
57. Tomlins SA, Rhodes DR, Perner S, Dhanasekaran SM, Mehra R, Sun XW, Varambally S, Cao X, Tchinda J, Kuefer R, Lee C, Montie JE, Shah RB, Pienta KJ, Rubin MA, Chinnaiyan AM. 2005. Recurrent fusion of *TMPRSS2* and ETS transcription factor genes in prostate cancer. Science 310:644–648. https://doi.org/10.1126/science.1117679.